



Surface PM_{2.5} Air Pollution in 2022 India:

Emission Updates, WRF-Chem Model Evaluation, and Source Attribution

Mi Zhou^{1,2}, Denise L. Mauzerall^{1,2}, Viswanath Velamuri³, Sri Harsha Kota³, Malini Nambiar², and Yuanyu Xie²

Correspondence to: Mi Zhou (miz@princeton.edu) and Denise L. Mauzerall (mauzerall@princeton.edu)

¹Department of Civil and Environmental Engineering, Princeton University, USA

²Center for Policy Research on Energy and the Environment, Princeton School of Public and International Affairs, Princeton University, USA

³Department of Civil and Environmental Engineering, Indian Institute of Technology Delhi, India



5

10

15



Abstract

India experiences some of the highest fine particulate matter (PM2.5) concentrations globally. Understanding the spatiotemporal variations of PM_{2.5} and its source attribution requires robust air quality modeling supported by up-to-date emission inventories. Here we present the first WRF-Chem model evaluation and source attribution analysis for India for 2022, supported by updates in sectoral emission inventories and model schemes. We incorporate an updated residential emission inventory reflecting recent transitions to cleaner fuels in Indian households and develop a plant-level inventory for Indian coal-fired power plants. Further major improvements include model updates to the secondary organic aerosol scheme and an improved representation of near-surface pollutant mixing. Collectively our improvements result in a simulation with annual PM_{2.5} bias of only 0.2±16.9 μg/m³ (0±31%) across 288 surface monitoring sites in South Asia. We find that, compared to earlier studies, in 2022 India's residential sector remained the dominant source of PM_{2.5} in the Indo-Gangetic Plain, but nationally ranked second in population-weighted (PW) mean PM_{2.5} concentrations contributing 15% (7.3 μg/m³). Instead, industrial emissions emerged as the largest domestic contributor to national PW mean PM_{2.5} (18%, 8.6 µg/m³), with urban hotspots including Delhi and Mumbai. The power sector contributions ranked third nationally (13%, 6.1 μg/m³) and was particularly influential in central India. Transboundary transport contributed more than any individual domestic source nationally (27%, 12.8 μg/m³). These findings highlight the benefits of India's partial residential sector transition toward cleaner fuels, while underscoring the growing consequence of industrial and power sector emissions that have limited pollution controls.



25

30

35

40

45

50

55



1 Introduction

Long-term exposure to elevated ambient fine particulate matter (PM_{2.5}) is a major risk factor for human health and premature mortality globally (Institute for Health Metrics and Evaluation, 2024). India has among the highest surface PM_{2.5} concentrations worldwide, leading to an estimated 1.0 to 2.1 million premature deaths annually (Lelieveld et al., 2015; Health Effects Institute, 2024). To address the severe air pollution challenges, the Indian government has proposed and implemented measures aimed at reducing emissions of PM_{2.5} and its precursors, including the National Clean Air Program (NCAP) launched in January 2019 (The Government of India, 2019). Despite an observed reduction in surface PM_{2.5} levels across India during 2018 to 2022, aided by favorable meteorology, annual PM_{2.5} pollution in ~80% of non-attainment cities with continuous monitors still exceeded the country's annual standard of 40 μ g/m³ in 2022 (Xie et al., 2024). In addition, future PM_{2.5} pollution in north India is projected to worsen under global warming (Zhang et al., 2023; Zhou et al., 2024). This highlights the need for strengthened mitigation measures. Effective regulation design and implementation depend on understanding spatiotemporal distributions of PM_{2.5} across India and the contribution of various emission sources. Given the complex interactions of atmospheric physical and chemical processes across India, robust emissions and air quality modeling are essential to address these questions.

Previous modeling studies have quantified the source contributions to India's annual ambient PM2.5 pollution levels during 2015 to 2019 (Conibear et al., 2018; Guo et al., 2018; Reddington et al., 2019; Singh et al., 2021; Pai et al., 2022; Chatterjee et al., 2023; Kumar et al., 2025; Venkataraman et al., 2018). Across these studies, the residential sector consistently emerged as the leading contributor to PM2.5 exposure nationwide, accounting for 21% to 52% of the national annual population-weighted (PW) mean PM_{2.5} concentrations, with the range reflecting whether transboundary transport of residential emissions from adjacent countries were attributed to the residential sector. This dominance stems from inefficient and incomplete small-scale combustion of solid fuels in households, which produces substantial primary PM2.5 emissions. In the literature, the power and industrial sectors were often among the largest national PM_{2.5} sources after the residential sector, but their relative importance varied across studies, depending on the anthropogenic emission inventory applied. The power sector has been the dominant source of sulfur dioxide (SO2, a key precursor of secondary inorganic PM2.5) emissions since 2015 (Venkataraman et al., 2018), primarily due to India's fast-growing electricity demand and heavy dependence on coal, with only about 3% of coal-based power plants equipped with flue gas desulfurization (FGD) systems in 2022 (National Environmental Engineering Research Institute, 2024). In addition, the industry sector was a major source of primary PM_{2.5} and SO₂ emissions in 2015, and its emissions were projected to continuously increase from 2015 to 2050 (Venkataraman et al., 2018). In addition to these anthropogenic sources within India, studies identified a 20-28% contribution from background (transboundary plus natural) sources to national mean PM_{2.5} in India in 2016 (Singh et al., 2021; Pai et al., 2022).

Amid India's fast development, surging energy demand, and ongoing air quality regulations, the more recent source contributions to PM_{2.5} concentrations across the country remains unclear. Specifically, the continued





growth of coal-based electricity generation in the power sector and the promotion of cleaner fuels in the residential sector have not been incorporated into existing PM_{2.5} attribution studies. In addition, previous PM_{2.5} modeling studies for India—excluding those projecting future changes—primarily focused on years before the NCAP baseline year of 2017, when relatively few surface PM_{2.5} measurement sites existed and thorough model evaluation was thus not possible (Schnell et al., 2018; Guo et al., 2018; Singh et al., 2021; Pai et al., 2022; Agarwal et al., 2024). Given the need for up-to-date source attribution studies to guide India's future air quality interventions (e.g., the next phase of the NCAP), more rigorous modeling studies with updated emissions and robust model evaluation that disentangle the source contributions to India's surface PM_{2.5} pollution in recent years are needed.

65

70

75

80

85

90

60

Here we present the first air quality modeling analysis for India using updated emissions for 2022, supported by key improvements in sectoral emission inventories and model schemes. We incorporate revised residential emissions that capture household transitions from solid fuels to liquefied petroleum gas (LPG), develop a refined plant-level inventory for coal-fired power generation, and update model treatments of secondary organic aerosol (SOA) formation and pollutant near-surface mixing. Using this enhanced inventory and model schemes, we conduct a rigorous evaluation of simulated PM_{2.5} concentrations against 288 surface PM_{2.5} measurements and satellite-derived aerosol optical depth (AOD) retrievals across India and adjacent regions. We then quantify the contributions of nine emission sources to surface PM_{2.5} pollution across India in 2022: eight domestic sources (six anthropogenic and two natural) and transboundary source (all sources combined as one), providing critical insights for targeted air quality policy interventions.

2 Methods

2.1 WRF-Chem model

We use a recent version of the Weather Research and Forecasting model coupled with Chemistry (WRF-Chem, version 4.6.1) primarily developed by the National Center for Atmospheric Research (NCAR) (Grell et al., 2005). WRF-Chem is a mesoscale air quality model that online couples atmospheric chemistry (including aerosols) and meteorology (Fast et al., 2006; Chapman et al., 2009), allowing the simulation of the aerosol feedback on regional meteorology that are particularly critical in regions with high aerosol loadings (Zhou et al., 2019; Sharma et al., 2023; Huang et al., 2023). WRF-Chem is thus widely used to simulate surface PM_{2.5} pollution over India (Govardhan et al., 2019; Agarwal et al., 2024; Venkataraman et al., 2024; Xie et al., 2024).

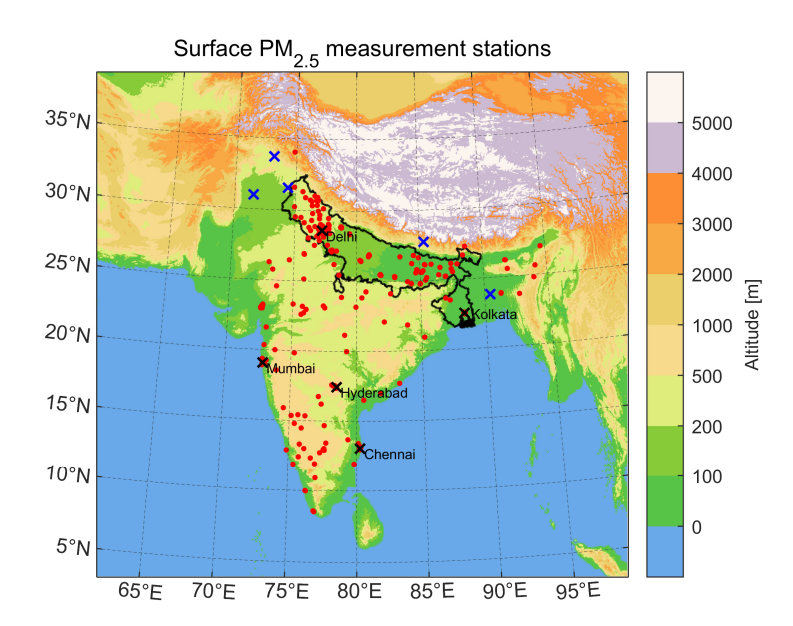
2.1.1 Model Configuration

We conduct simulations for 2022, the most recent year with available emission inventories for India (**Section 2.2**), using one month to represent each season: January for winter, April for pre-monsoon, July for monsoon, and October for post-monsoon. We use a single domain covering India and adjacent regions (57-103° E, 4-39°





N) with a horizontal resolution of 27 km² (**Figure 1**). There are 37 vertical layers extending from the surface to 50 hPa, with 10 to 15 layers below 1000m above ground level, depending on local terrain heights. For meteorological initial and lateral boundary conditions, we use the hourly ERA5 climate reanalysis dataset at $0.25^{\circ} \times 0.25^{\circ}$ resolution. To prevent drifting effects in simulated meteorological fields, we reinitialize WRF-Chem meteorology with ERA5 every 48 hours, following our previous studies (Zhou et al., 2022; Xie et al., 2024). The chemical initial and boundary conditions are provided by the 6-hour output from the Whole Atmosphere Community Climate Model (WACCM) (Gettelman et al., 2019; Emmons et al., 2020).



100

105

Figure 1. WRF-Chem modeling domain and surface PM_{2.5} measurement stations utilized in this study. The base map shows the WRF-Chem modeling domain, with colors representing the terrain height in the model. The 288 surface PM_{2.5} measurement sites used in this study are marked as follows: Red dots represent the continuous monitoring stations from the Indian Central Pollution Control Board (CPCB) network; the black and blue crosses represent the stations from U.S. Air Now network in India and adjacent countries, respectively. Thick black lines represent the boundary of the Indo-Gangetic Plain (IGP), which includes Delhi, Punjab, Haryana, Uttar Pradesh, Bihar, and West Bengal. We also label the five major cities of Delhi, Mumbai, Kolkata, Hyderabad, and Chennai, where U.S. Air Now PM_{2.5} measurements were available in India.

110

We configure WRF-Chem with the following chemical schemes: the Carbon Bond Mechanism Z (CBMZ) gas-phase chemistry scheme (Zaveri and Peters, 1999), and the 4-bin version of the MOdel for Simulating Aerosol Interactions and Chemistry (MOSAIC) aerosol scheme with aqueous chemistry (Zaveri et al., 2008). The selected MOSAIC scheme simulates major aerosol species, including primary organic aerosols (POA), black carbon (BC), sulfate (SO_4^{2-}), nitrate (NO_3^{-}), ammonium (NH_4^{+}), sodium (Na^{+}), chloride (CI^{-}), and other inorganic



125

130

135

145

150



aerosols (OIN, including both natural dust and anthropogenic combustion and non-combustion dust). Each aerosol species is distributed across four size bins, with the first three bins (diameters ≤ 2.5 μm) contributing to PM_{2.5} dry mass. Aerosols are assumed to be internally mixed inside each bin for optical property calculations. Under this configuration, the water uptake and hygroscopic growth properties of aerosols are calculated based on the bulk composition of the internally mixed particles (Zaveri et al., 2008). Configurations for physical schemes are provided in **Supplementary Information 1.1**.

Natural emissions of dust and biogenic Non-Methane Volatile Organic Compounds (NMVOCs) are calculated online within WRF-Chem. For dust emissions, we use the Goddard Chemistry Aerosol Radiation and Transport (GOCART) dust module (Ginoux et al., 2001). The GOCART dust emission scheme is widely used in aerosol modeling due to its relatively simple input requirements. Specifically, the GOCART scheme calculates dust emission fluxes using surface erodibility, 10-meter wind speed, threshold soil moisture, and threshold wind speed, distributing dust aerosols into five size bins that partially overlap with the MOSAIC aerosol scheme's PM_{2.5} bins. For biogenic NMVOCs, we use the Model of Emissions of Gases and Aerosols from Nature (MEGAN, version 2.06) (Guenther et al., 2006). MEGAN uses leaf area index (LAI), plant functional types (PFTs), and WRF-Chem-simulated meteorology to calculate emissions for 134 chemical species, which are subsequently mapped into the CBMZ gas-phase mechanism. Anthropogenic emissions, including emissions of open burning are described in Section 2.2.

Based on the model configuration, PM_{2.5} dry mass in WRF-Chem is calculated using Equation 1:

 $PM_{2.5} = \sum_{i=1}^{i=3} (POA_i + BC_i + OIN_i + SO_{4-i}^{2-} + NO_{3i}^{-} + NH_{4i}^{+} + Na_i + Cl_i)$ (1)

Here, *i* indicates the aerosol bin used in WRF-Chem.

140 2.1.2 Model Updates

We implement the simple SOA scheme from the GEOS-Chem global chemistry transport model into WRF-Chem 4.6.1, as the selected WRF-Chem chemical option treats POA as non-volatile and does not include SOA. The simple SOA scheme uses a fixed-yield approach to estimate SOA and SOA precursor (SOAP) emissions from biogenic and combustion sources. For biogenic sources, SOA (SOAP) mass yields are assumed to be 1.5% (1.5%) from isoprene and 5% (5%) from both monoterpenes and sesquiterpenes. For combustion sources, no SOA is directly emitted. However, SOAP mass yields are assumed to be 1.3% (6.9%) from biomass (fossil fuel) combustion carbon monoxide (CO). Designed as a computationally efficient alternative, the simple SOA scheme approximates SOA concentrations without mechanistically modeling the formation and fate of individual aerosol species or explicit thermodynamic partitioning (Pai et al., 2020). The simple SOA scheme has demonstrated performance comparable to more complex, process-based SOA schemes (Pai et al., 2020; Miao et al., 2021). For simplicity, the predicted SOA mass from the simple SOA scheme is added to the POA variable to represent total



160

165

170

175

180



organic aerosols in the model, as shown in Equation 1.

We improve near-surface mixing of chemical species by setting a minimum exchange coefficient for air pollutants in the selected boundary layer scheme, following a previous study that found WRF-Chem's weak nighttime mixing led to overestimated diurnal variations of PM_{2.5} (Du et al., 2020).

2.2 Anthropogenic emissions

2.2.1 Adoption of existing 2022 emission inventories

We use the most recent release of two global emission inventories for our 2022 WRF-Chem simulation: the Community Emissions Data System (CEDS, version 2024-07-08) and the Emissions Database for Global Atmospheric Research (EDGAR, version 8.1). Both inventories provide gridded emissions for years until 2022 and are widely used for air quality research. We adopt monthly gaseous emissions of sulfur dioxide (SO₂), nitrogen oxides (NO_x), ammonia (NH₃), CO, and NMVOCs in 2022 from CEDS at 0.5°×0.5° resolution (Hoesly et al., 2018). In addition, we obtain monthly particulate matter emissions of primary organic carbon (POC), BC, primary PM_{2.5}, and PM₁₀ emissions in 2022 from EDGAR at 0.1°×0.1° resolution (Crippa et al., 2018), as CEDS does not provide primary PM_{2.5} and PM₁₀ emissions. We spatially interpolate CEDS and EDGAR inventories to the 27-km resolution WRF-Chem grid using a mass-conservative method. We use the satellite-derived daily Fire INventory from NCAR (FINN, version 2.5.1) to represent open burning emissions of agricultural and municipal waste, as well as smoke emissions from wildfires (Wiedinmyer et al., 2023). To avoid double counting, we exclude open burning emissions from the global inventories described above when they already include this source.

To better capture India's recent increasing displacement of solid fuels by LPG for clean residential energy use (The Government of India, 2019), we adopt a 2022 emission inventory developed at the Indian Institute of Technology Delhi. This new residential inventory applies regression analysis to evaluate residential fuel usage, considering recent changes in consumption patterns and updated data on cleaner fuels (Velamuri et al., 2024). Thus reductions in emissions from the residential sector are better represented than in the flat residential emission trends provided in EDGAR and CEDS from 2015-2022 (**Figure 2**). Specifically, we adjust India's residential PM_{2.5}, SO₂, and NO_x emissions to align with state-level totals from this new residential inventory. In addition, we scale residential emissions of OC, BC, and CO in each Indian state using the factor calculated as the ratio of residential PM_{2.5} emissions from the new inventory to those from EDGAR. We retain the original spatial patterns for all these scaled species. We provide a detailed comparison between residential emissions from the current global inventories and our updated inventory in **Section 3.1**.

Then, we replace the PM_{2.5}, SO₂, and NO_x emissions from coal-fired power plants in the updated inventory with a new national emission inventory for coal-fired power plants in India for 2022, which is detailed in section **2.2.2**.

185



200

205

210

215

220

225



In addition to these major updates to the emissions from India's residential and power sectors, we scale India's transportation-related PM_{2.5} and coarse PM (PM_{coarse}, defined as particles with diameters > 2.5 μm and ≤ 10 μm) emissions to match the state-level totals from a 2022 road dust emission inventory (Katiyar et al., 2024). This adjustment is motivated by our finding that transportation PM_{2.5} emissions in EDGAR (i.e., 0.11 Tg across India in 2022) are underestimated compared with this locally-developed inventory in India (i.e., 0.33 Tg). Similarly, transportation PM_{coarse} emissions in EDGAR were only 0.01 Tg across India in 2022, significantly lower than the 1.04 Tg estimated by the recent Indian inventory. The discrepancy likely reflects EDGAR's omission of fugitive road dust PM_{2.5} emissions.

We provide details on aerosol mapping from EDGAR to WRF-Chem and on vertical allocation of emissions in **Supplementary Information 1.2-1.3**.

2.2.2 Development of new 2022 coal-fired power plant emission inventory for India

We construct a new national emission inventory for coal-fired power plants in India in 2022, focusing on major air pollutants of SO₂, NO_x, and PM_{2.5}. The development of this inventory involves three major steps: (1) compiling and cross-checking unit-level information from multiple databases; (2) estimating plant-level emission factors based on a fuel linkage database linking coal used at specific plants to coal source regions, coal composition information, and a document estimating emissions factors from coal composition (U.S. Environmental Protection Agency); and (3) utilizing plant-level electricity generation and coal consumption data from reports from the Central Electricity Authority (CEA) of India. Each of these steps is detailed in the following paragraphs.

We collect unit-level information from the Global Energy Monitor's (GEM)'s coal power plant database for July 2022. To align with India's central government data, as reflected in the Vasudha Foundation's datasets (The National Institution for Transforming India Aayog, 2025), we include all operating units from the GEM database. For captive units, we only include those documented by Vasudha. This results in a total of 210.6 GW in generation capacity, which matches the coal and lignite capacity reported by the CEA in July 2022. We retrieve the unit location from the GEM database. For units listed with "approximate" location coordinates in the GEM database, we update their coordinates using Google Earth. We replace the heating rate in the GEM database with a machine-learning-developed, measurement-constrained database (Ding et al., 2024).

We collect coal composition data for nine domestic coal source states and three imported coal regions (Australia, South Africa, and Indonesia) through a literature review. We then convert the carbon, sulfur, and ash content of coal into uncontrolled emission factors for SO₂ and PM_{2.5} under various firing configurations for both bituminous and subbituminous coal based on a report (U.S. Environmental Protection Agency). In addition, the

report provides NO_x emission factors that are independent of nitrogen content in the coal. Based on this



240

245

255

260



information, we establish region-specific uncontrolled emission factors for both domestic coal and imported coal used in India's power plants (**Supplementary Table 1**). We average data for a given region if multiple coal composition data is found. We assume no variation in coal composition within a given coal source region. Plant-level fuel linkage dataset are obtained from multiple data sources (The National Institution for Transforming India Aayog, 2025), which matches each plant with one or more coal source regions. Finally, we estimate plant-level emission factors for air pollutants, using **Equation 2**.

$$EF_{i,s} = \sum_{r=1}^{n} EF_{r,s} * F_{i,r}$$
 (2)

Where $EF_{i,s}$ is the emission factor (g pollutant/kg coal) for power plant i and species s; $EF_{r,s}$ is the emission factor (g pollutant/kg coal) of coal for source region r and species s; $F_{i,r}$ is the fraction of coal supplied at plant i that is sourced from region r.

We retrieve daily plant-level coal consumption reports from the CEA for the calendar year 2022 and aggregate data by month. In addition, we retrieve monthly plant-level electricity generation reports from the CEA for the same year. While generation data is available for all plants throughout the year, the coal consumption data is missing for some plants. For plants with missing monthly coal consumption data, we estimate the missing values by applying the plant's generation-to-coal consumption ratio, averaged from months where both generation and coal consumption data are available. For plants with no coal consumption data for the entire year, we estimate the coal consumption using the reported generation, coal heating value, and heating rate using **Equation 3**:

$$C_{i,j} = G_{i,j} * HR_i/TV_i \tag{3}$$

Where $C_{i,j}$ is the monthly coal consumption (tons) for power plant i and month j; $G_{i,j}$ is the monthly electricity generation (MWh) for power plant i and month j; HR_i is the heating rate (MJ/kWh) for plant i, which represents the plant thermal efficiency; TV_i is the thermal value (MJ/kg coal) of coal used in plant i.

Finally, we estimate the monthly total emissions for air pollutants for each plant, using Equation 4.

$$E_{i,i,s} = C_{i,i} * EF_{i,s} * (1 - \eta_s) \tag{4}$$

Where $E_{i,i,s}$ is the monthly total emissions (tons) for power plant i, month j, and species s; $C_{i,j}$ is the monthly coal consumption (tons) for power plant i and month j; $E_{i,s}$ is the emission factor (kg pollutant/ton coal) of coal for plant i and species s; η_s is the removal efficiency for air pollutant species s, and we assume a 90% removal rate (η =0.9) for PM_{2.5} and no end-of-pipe controls for SO₂ and NO_x (η =0) following previous studies (Sengupta et al., 2022; Singh et al., 2024). This assumption is supported by a recent report which documents that only 3.2%





of coal-based power plants in India have installed Flue Gas Desulfurization (FGD) systems and does not mention the installation of NO_x control devices (National Environmental Engineering Research Institute, 2024).

265

We do not account for NO_x emission from gas plant operation in 2022. According to the Indian Petroleum and Natural Gas Statistics 2022–23, gas consumption for this fiscal year was ~8 billion m³. Using the gas plant NO_x emission factors from the USEPA report, we estimate the total NO_x emissions from gas plant to range from 0.01 to 0.04 Tg/year, which is far lower than those from coal-fired power plants (i.e., 4.56 Tg/year).

270

275

280

285

290

2.3 Measurement data for model evaluation

2.3.1 Surface PM_{2.5} measurements

To evaluate the model performance, we compare simulated PM_{2.5} dry mass concentrations with surface observations from the India Central Pollution Control Board (CPCB) continuous monitoring network and the US AirNow network in South Asia (**Figure 1**). We initially retrieve hourly data from 510 measurement stations within the WRF-Chem modeling domain and apply rigorous quality control procedures to filter out outliers and identical consecutive values, as documented in our previous publications (Zhou et al., 2024; Xie et al., 2024). Measurement stations with at least 80% valid hourly data in a given model evaluation period (e.g., January 2022) after quality control are used to evaluate the WRF-Chem model. This criterion excludes 223 stations and retains 288 stations for analysis. Multiple measurements within a single WRF-Chem grid cell are averaged before comparison with model output.

2.3.2 Satellite AOD measurements

We obtain Aerosol Optical Depth (AOD) from the Multi-Angle Implementation of Atmospheric Correction (MAIAC) algorithm, which provides AOD at a 1-km spatial resolution globally over land and coastal regions (Lyapustin et al., 2018). The radiances used in the retrieval are measured by the twin Moderate Resolution Imaging Spectroradiometer (MODIS) instruments onboard the Terra and Aqua satellites. Terra follows a descending orbit with an equatorial crossing at 10:30 Local Time (LT), while Aqua follows an ascending orbit with an equatorial crossing at 13:30 LT. For model evaluation, we interpolate the satellite AOD to the WRF-Chem resolution of 27 km², and compare it with the model results averaged from 10:00 to 14:00 LT each day for each grid box. In addition, WRF-Chem calculates AOD at 300 nm, 400 nm, 600 nm, and 1000 nm wavelengths, and the model interpolates AOD to 550 nm for diagnostic output using the Ångström power law, making it consistent with the MAIAC product.

2.3.3 Population dataset and Population-Weighted (PW) mean PM_{2.5} concentration

We obtain gridded 2015 population from the Global Population for the World dataset (version 4) and scale those values to reported total population in India in 2022. PW mean PM_{2.5} concentrations in a given region is calculated using **Equation 5**.





300
$$PWPM_{2.5} = \sum_{i=1}^{i=n} (PM2_{2.5,i} * POP_i) / \sum_{i=1}^{i=n} (POP_i)$$
 (5)

Where $PM_{2.5,i}$ and POP_i are the annual mean $PM_{2.5}$ concentration (from the WRF-Chem baseline simulation) and total population in grid i, respectively; n is the number of model grids in a given region.

2.4 WRF-Chem Simulation

We conduct a baseline simulation using the model configurations described in **Section 2.1** and the updated anthropogenic emission inventory described in **Section 2.2**. We perform a thorough model evaluation against PM_{2.5} and AOD observations in **Section 2.3** that establishes the robustness of model results.

To attribute surface PM_{2.5} concentrations to specific sources, we next conduct a series of additional WRF-Chem simulations in which emissions from individual sources inside and outside India are sequentially zeroed out. We individually remove six domestic anthropogenic sectors within India (i.e., power, industry, residential, transportation, open burning, and agriculture emissions), two natural sources within India (i.e., dust and biogenic emissions), and transboundary emission sources from outside India (i.e., natural and anthropogenic emissions). We provide a summary of emission scenarios for all WRF-Chem simulations in **Table 1**.

Table 1. Emission scenarios for WRF-Chem simulations conducted in this study

Scenarios	Domestic Sources (Emissions inside India)			Transboundary Sources	
	Anthropogenic *	Dust ¶	Biogenic ¶	(Emissions outside India) †	
Baseline	On	On	On	On	
POW_{off}	Power sector <i>off</i> ‡		On	On	
IND_{off}	Industry sector off [‡]				
RESoff	Residential sector off [‡]	On			
TRA _{off}	Transportation sector off [‡]	Oli			
AGR_{off}	Agriculture sector off [‡]				
FIRE _{off}	Open burning <i>off</i> ‡				
$\mathrm{DST}_{\mathrm{off}}$	On	Off	On	On	
$BVOC_{off}$	On	On	Off	On	
TBDY _{off}	On	On	On	Off	

^{*}This includes emissions from six source sectors within India: power, industry, residential, transportation, agriculture (excluding open burning), and open burning.

[¶]We modify WRF-Chem to enable grid-level customization to turn dust and biogenic emission modules on and off.

This includes both anthropogenic and natural emissions (i.e., dust and biogenic) originating outside of India but within the WRF-Chem modeling domain, as well as the long-range transport of pollutants from regions beyond the WRF-Chem domain (i.e., the chemical boundary conditions for the model derived from the Whole Atmosphere Community Climate Model).

315

305

310





*All other sectors' emissions are kept unchanged as the baseline scenario.

325

330

The contribution of each source is first estimated by subtracting the results of the source-zeroed simulation from those of the baseline simulation, using **Equation 6**. However, due to strong non-linearities in the relationship between partial emission reductions (i.e., less than 100%) and resulting decreases in PM_{2.5} concentrations—primarily driven by secondary PM_{2.5} formation (Liu et al., 2021) and aerosol-meteorology feedbacks (Zhou et al., 2019)—the sum of individual source contributions does not equal the total concentration in the baseline simulation. To address this disparity, we apply a scaling factor to each source's contribution, based on the ratio of baseline concentration to the summed contributions at each WRF-Chem grid cell for PM_{2.5} and its components, using **Equation 7**. This ensures that the sum of individual source contributions equals the total concentration in the baseline simulation for each WRF-Chem grid.

335

$$Contrib_{chem,i} = C_{chem,baseline} - C_{chem,i-off}$$
 (6)

$$Contrib_{scaled,var,i} = Cont_{var,i} * \frac{C_{var,baseline}}{\sum_{i=1}^{9} Cont_{var,i}}$$
(7)

340

Here, $Contrib_{chem,i}$ represents the source attribution (in concentration units) of chemical species chem to the i^{th} emission source; $C_{chem,baseline}$ and $C_{chem,i-off}$ are the WRF-Chem simulated concentrations of chemical species chem in the baseline simulation and in the simulation where the i^{th} emission source is turned off, respectively; $Contrib_{scaled,chem,i}$ is the scaled source attribution (in concentration units) of variable chem to the i^{th} emission source.

345

350

355

3 Results

In this section, we first compare annual national and sectoral anthropogenic emissions of PM_{2.5} and key precursors in India from 2015 to 2022, comparing multiple global inventories and our updated merged 2022 inventory (**Section 3.1**). We then evaluate the performance of the WRF-Chem model using ground-based PM_{2.5} measurements and satellite-derived aerosol optical depth (AOD) (**Section 3.2**). Last, we use the model to assess the spatial distribution of PM_{2.5} pollution in 2022 and quantify contributions from major emission sources to both total PM_{2.5} and PM_{2.5} components (**Section 3.3-3.4**).

3.1 Comparison of annual anthropogenic emissions of PM2.5 and key precursors in India

We present annual national total and sectoral emissions for SO₂, NO_x (as NO₂), and PM_{2.5} in India from 2015 to 2022 (**Figure 2**), showing results from five inventories: our updated 2022 inventory, the Speciated MultipOllutant Generator (SMoG) 2015 inventory developed in Indian Institute of Technology (IIT) Bombay (Venkataraman et al., 2018), and three widely used global inventories (recent releases)—CEDS (released on 2024-07-08), EDGAR (version 8.1, released in 2024), and Hemispheric Transport of Air Pollution (HTAP,



365

370



version 3.1, released in 2025) (Hoesly et al., 2018; Crippa et al., 2018; Guizzardi et al., 2025). For global inventories, while CEDS and EDGAR provide emissions up to 2022, HTAP extends only through 2020. For India, HTAP adopts the Regional Emission inventory in ASia (REAS, version 3.2.1 (Kurokawa and Ohara, 2020)) for 2015 and applies country-sector-pollutant-specific emission trends derived from EDGAR to estimate emissions from 2016 to 2020.

Annual primary $PM_{2.5}$ emissions in India, reported only by EDGAR (2015-2022), HTAP (2015-2020), and SMoG (2015), exhibit interannual variations, with emissions increasing from 2015 to 2018, declining to 2020, and rising again thereafter. Specifically, EDGAR reports a total $PM_{2.5}$ emission of 4.3 Tg in 2022, while HTAP reports 5.0 Tg for 2020, its latest available year. The cross-inventory uncertainty for annual $PM_{2.5}$ emissions (calculated annually as the highest emission minus the lowest emission, divided by the averaged emission) from 2015 to 2020 is $24\pm2\%$. The residential and industrial sectors were two leading contributors to total $PM_{2.5}$ emissions in India, accounting for $42\pm2\%$ and $41\pm5\%$ of total emissions, respectively.

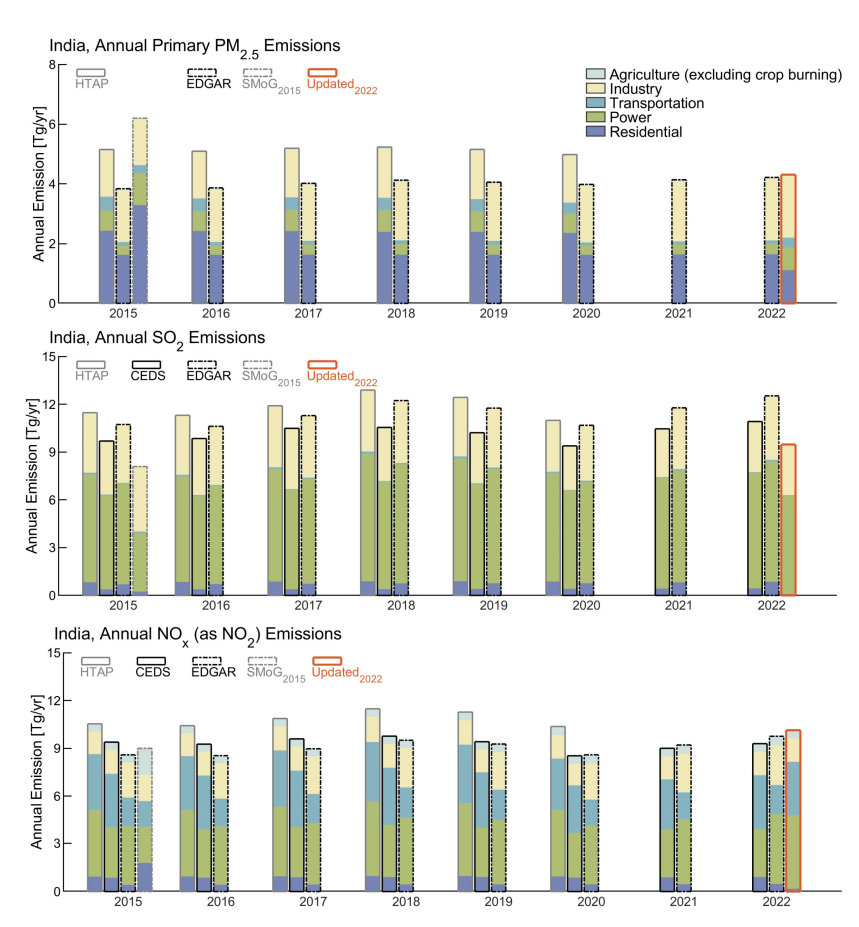


Figure 2. Comparison of annual anthropogenic sectoral total emissions over India among three global



375

380

385

390

395

400

405

410



inventories, one regional 2015 inventory, and our updated 2022 inventory. For each country and species, CEDS_{v2024-07-08}, EDGAR_{v8.1}, and HTAP_{v3.1} report sectoral total emission across 59, 32, and 16 detailed sectors, respectively. Those detailed sectors are aggregated into five widely used sectors: power, industry, residential, transportation, and agriculture. In this figure, because CEDS_{v2024-07-08} does not include open burning of agricultural waste and wildfire, we exclude it from the agricultural sector emissions in EDGAR_{v8.1} and HTAP_{v3.1} to enable direct comparison among the inventories. Note that CEDS_{v2024-07-08} does not provide primary PM_{2.5} emissions, and HTAP_{v3.1} extends only until 2020. Details on the updated inventory are provided in Section 2.1.

For annual total SO₂ emissions, all three global inventories indicate a similar emission trend from 2015 to 2020, showing an increase from 10.6 ± 0.9 Tg in 2015 to a peak of 11.8 ± 1.2 Tg in 2018, followed by a reduction to 10.3 ± 0.8 Tg in 2020 due to COVID lockdown. After 2020, the CEDS and EDGAR inventories report increases in annual total SO₂ emissions from 9.4 Tg and 10.7 Tg in 2020 to 10.9 Tg and 12.5 Tg in 2022, respectively. The cross-inventory uncertainty for annual SO₂ emissions is $15\pm3\%$ from 2015 to 2022. The power sector consistently dominates SO₂ emissions in India from 2015 to 2022, accounting for $61\pm2\%$ of total emissions across inventories (**Supplementary Table 2**). This dominance is driven by India's growing electricity consumption (e.g., an increase of 86% from 2010 to 2022) and continued heavy reliance on coal-fired power generation (e.g., 72% in 2022), along with limited implementation of end-of-pipe pollution controls (Kumar and Dahiya, 2023). The industry and residential sectors contribute $32\pm2\%$ and $6\pm0\%$, respectively, to total SO₂ emissions in India over the same period.

Similarly, annual total NO_x emissions in India increased from 9.5 ± 1.0 Tg in 2015 to 10.2 ± 1.1 Tg in 2018, then declined to 9.1 ± 1.0 Tg by 2020 according to all three global inventories. Post-2020, the CEDS and EDGAR inventories show increases in annual total NO_x emissions from 8.5 Tg and 8.6 Tg in 2020 to 9.3 Tg and 9.8 Tg in 2022, respectively. The power sector remains the largest contributor to NO_x emissions over the period of 2015 to 2022 in all inventories, accounting for $39\pm0\%$ of the total, followed by the transportation ($29\pm1\%$), industry ($19\pm1\%$), and residential ($8\pm0\%$) sectors. The inventory for annual NO_x emissions is $16\pm8\%$ from 2015 to 2022 across inventories.

Solid fuel had been historically widely used in India's residential sector, such as biomass for residential cooking and kerosene for lighting, which leads to high PM_{2.5} emission due to their inefficient and incomplete combustion (Chowdhury et al., 2019). The residential sector has recently benefited from mitigation efforts under the NCAP which has promoted the use of liquified petroleum gas (LPG) as a cleaner fuel replacing solid fuels (Bhaskar, 2019). This clean energy transition in the residential sector is not captured by any of the global inventories, in which residential emissions remain largely unchanged after 2017 (**Figure 2**). Therefore, we adopted a recently developed residential emission inventory that accounts for recent consumption pattern changes and cleaner fuel adoption in 2022 (Velamuri et al., 2024). As a result of incorporating the updated residential inventory, annual total residential emissions are reduced by 0.5 Tg for primary PM_{2.5} (33% relative



445



to EDGAR), reduced by 0.4 Tg for SO_2 (82% relative to CEDS), and reduced by 0.7 Tg for NO_x (80% relative to CEDS).

415 In addition to update the residential emissions, we replace power sector emissions with our coal-fired power plant emission inventory described in Section 2.2.2. Our coal-fired plant emission inventory covers all operating units regulated by India's Central Electricity Authority (CEA), using detailed plant-level generation reports archived by the CEA to improve the accuracy of activity data. We estimate annual total emissions from coal-fired power generation across India in 2022 to be 6.2±1.5 Tg for SO₂, 4.6±0.3 Tg for NO_x, and 0.8±0.1 Tg 420 for primary PM2.5, with the range reflecting uncertainties in emission factors without mitigation as reflected in the literature (Supplementary Table 1). These total emissions, along with the estimated emission factors per unit of electricity generated, are comparable to those reported in four earlier studies focused on India's coal-fired power plant emissions (Guttikunda and Jawahar, 2014; Cropper et al., 2021; Singh et al., 2024; Velamuri et al., 2024) (Supplementary Table 3). In addition, the spatial distributions of gridded power plant 425 emissions among CEDS, EDGAR, and our inventory are similar (Supplementary Figure 1). As a result of incorporating our coal plant inventory, annual total emissions for the power sector are increased by 0.4 Tg for PM_{2.5} (90% relative to EDGAR), reduced by 0.6 Tg for SO₂ (9% relative to CEDS), and increased by 0.4 Tg for NO_x (10% relative to CEDS). The adoption of India-specific emission factors (Supplementary Table 1), informed by a literature review of India's high-ash coal, may explain why our estimates of primary PM2.5 430 emissions are substantially higher than those from EDGAR. A 2019 emission inventory developed by multiple Indian institutions reported an even higher annual primary PM_{2.5} emission of 1.7 Tg from the power sector (Venkataraman et al., 2024).

In 2022, our updated emission inventory reports India total emissions at 9.5 Tg for SO₂, 10.1 Tg for NO_x, and 4.3 Tg for primary PM_{2.5}. Compared with existing global inventories in 2022, our total SO₂ emissions are 1.4 Tg (13% relative to CEDS) lower, while total PM_{2.5} and NO_x emissions are 0.04 Tg (1% relative to EDGAR) and 0.8 Tg (9% relative to CEDS) higher, respectively. These differences result from the updates in emissions from the residential, power, and transportation (i.e., road dust) sectors in 2022.

440 3.2 Model evaluation for surface PM_{2.5} and aerosol optical depth (AOD)

The improved WRF-Chem simulations capture the spatial distribution of annual mean surface $PM_{2.5}$ concentrations (calculated as the mean of January, April, July and October means) across India and adjacent regions well, achieving a Pearson correlation coefficient (R) of 0.71 between modeled and observed concentrations (**Figure 3**). Annual model bias across the entire domain (116 model grids and 288 measurement sites) is $0.2\pm16.9~\mu\text{g/m}^3$ ($0\pm31\%$). Model biases in annual mean surface $PM_{2.5}$ are within $\pm10~\mu\text{g/m}^3$ in 57% of the WRF-Chem grids which have measurement sites, whereas biases exceed $\pm30~\mu\text{g/m}^3$ in 9% of these grids. Across the Indo-Gangetic Plain (IGP), the region with the most severe $PM_{2.5}$ pollution in India, simulated annual mean surface $PM_{2.5}$ concentrations differ from observed concentrations by $-1.9\pm21.2~\mu\text{g/m}^3$ ($3\pm31\%$).





455

460

465

Specifically, in Delhi, the modeled annual mean surface $PM_{2.5}$ concentration (100.2 $\mu g/m^3$) is virtually the same as the observed mean (100.7 $\mu g/m^3$). These results indicate the models' ability to reproduce the spatial pattern of annual mean surface $PM_{2.5}$ levels across India and nearby regions in 2022, providing large improvements over previous air quality modeling studies for India (Conibear et al., 2018; Reddington et al., 2019; Singh et al., 2021; Pai et al., 2022). Model simulations using the global emission inventories without improvements for Indian sectoral emissions and without improved near-surface mixing of pollutants show a significant overestimation of annual $PM_{2.5}$ by 23.0 ± 29.0 $\mu g/m^3$ (42 $\pm53\%$) across the domain and by 92.5 ± 40.9 $\mu g/m^3$ (92 $\pm41\%$) in Delhi (The 'Default' Simulation in **Figure 4**).

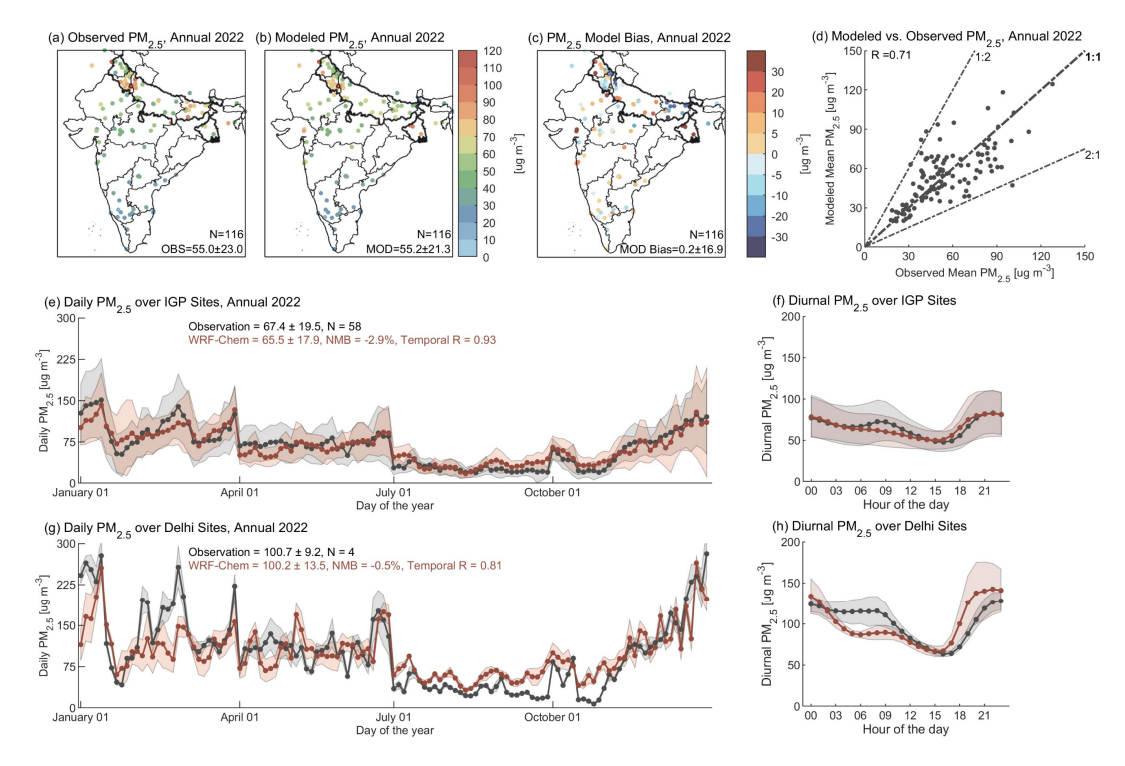


Figure 3. Comparison of observed and modeled surface $PM_{2.5}$ concentrations in 2022. Measurement stations with at least 80% valid hourly data during the four-month period (January, April, July, and October) are selected. Multiple measurements within a single WRF-Chem grid cell are averaged before comparison with WRF-Chem. a-d, comparison of annual mean surface $PM_{2.5}$ concentrations between observations (OBS) and model simulations (MOD). Annual value is estimated by averaging $PM_{2.5}$ concentrations during the four-month period. In a-c, N denotes the number of grid cells used for evaluation, and the other numbers represent the mean \pm one standard deviation across all grid cells. The thick black line denotes the boundary of the Indo-Gangetic Plain (IGP). In d, R is the Pearson correlation coefficient between observed and modeled annual mean concentrations across all grid cells. e and g, comparison of daily mean surface $PM_{2.5}$ concentrations between observations and WRF-Chem simulations in the IGP



475

480

485



(e) and Delhi (g). f and h are the same as e and g, but for annual mean PM_{2.5} diurnal variations. In e-h, red and black lines represent PM_{2.5} concentrations for observations and simulations, respectively, averaged across available grid cells in each region noted in the panel, with shaded areas indicating one standard deviation. Temporal R is the Pearson correlation coefficient between the red and black lines in each panel. See **Supplementary Table 4** for PM_{2.5} model performance at state level.

Beyond annual averages, WRF-Chem also effectively captures daily PM_{2.5} variations throughout the fourmonth period (**Figure 3e-h**). In the IGP and Delhi, the Pearson correlation coefficients between modeled and observed regional mean daily PM_{2.5} concentrations are 0.93 and 0.81, respectively. In addition, the twin-peak pattern in diurnal PM_{2.5} concentrations are well reproduced by WRF-Chem, though the morning peak in Delhi is underestimated. In contrast, model simulations without the emission and near-surface mixing updates show much stronger diurnal variability in hourly PM_{2.5} concentrations than the observation, resulting from overestimated local emission fluxes and insufficient nighttime near-surface mixing (**Figure 4**).

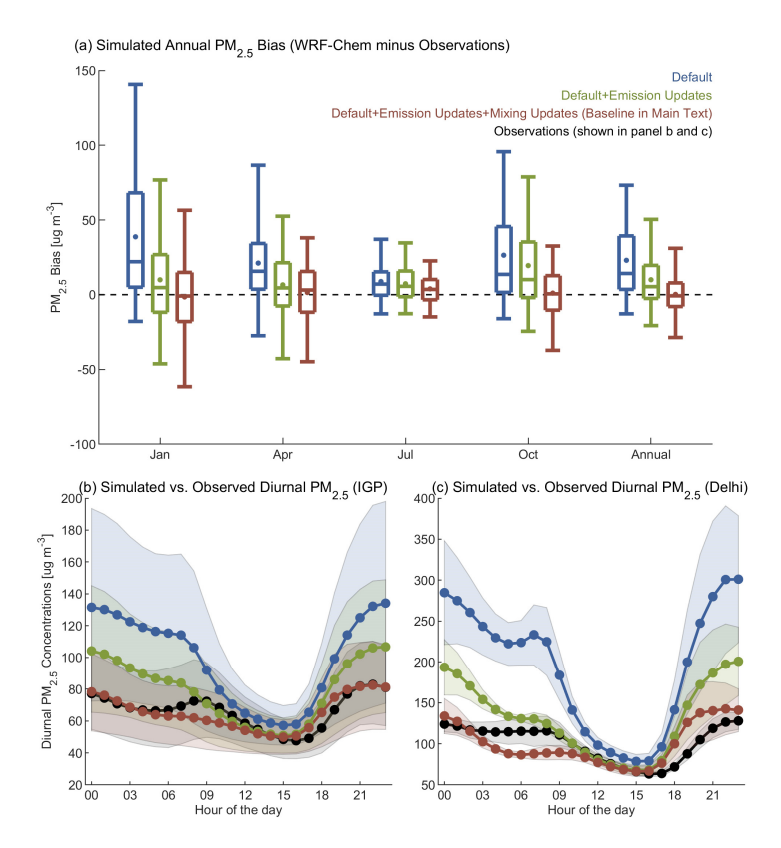


Figure 4. Comparison of PM_{2.5} performances among three emission and model configurations in 2022. The configurations are: (1) Default (in blue)— official WRF-Chem v4.6.1 with the GEOS-Chem simple SOA scheme, driven by the standard CEDS and EDGAR inventories as described in Section 2.2.1; (2) Default + Emission Updates





(in green)— configuration (1) plus sectoral updates for the residential and power sectors, as well as road dust, as described in **Sections 2.2.1** and **2.2.2**; (3) Default + Emission Updates + Mixing Updates (in red)— configuration (2) plus improved near-surface mixing of chemical species, this configuration is adopted by the Baseline simulation as mentioned in **Table 1** and **Figures 3** and **5**. Model performance is evaluated using (a) monthly and annual mean bias across the entire domain, and (b–c) annual mean PM_{2.5} diurnal patterns for the Indo-Gangetic Plain (IGP) and Delhi, respectively. In **a**, box-whisker plots demonstrate the distribution of PM_{2.5} model bias across the entire domain simulated by three configurations. The boxes denote the 25th, 50th, and 75th percentiles, and the whiskers denote the 5th and 95th percentiles of PM_{2.5} bias. In b-c, shaded areas indicate one standard deviation across available grid cells in each region noted in the panel.

495

500

505

510

515

520

490

Despite the good model performance of the baseline simulation discussed above, notable biases remain in several regions (Figure 3b). Specifically, modeled annual mean surface PM_{2.5} concentrations exceed observations by more than 30 µg/m³ in West Bengal (e.g., Kolkata) and a few stations in Gujarat, Punjab, and Rajasthan, while modeled concentrations underestimate observations by more than 30 μg/m³ in a few stations in Bihar and Uttar Pradesh. We summarize the state-level model performance in Supplementary Table 4. We find the largest negative model bias in annual mean surface PM_{2.5} concentrations in Bihar (-19±12 µg/m³, -23±17%). Out of 10 WRF-Chem grids in Bihar containing measurement stations, 9 grids underestimate PM2.5, with 2 grids underestimating by more than 30 μg/m³. In contrast, the largest positive model bias occurs in West Bengal, where modeled annual mean surface PM_{2.5} concentrations exceed observations by 32±19 µg/m³ (61±47%). Model biases in January play a dominant role in these annual biases, contributing, on average, 51% (10 μg/m³) of the annual negative bias in Bihar and 57% (18 µg/m³) of the annual positive bias in West Bengal. However, PM_{2.5} concentrations observed at CPCB stations in Kolkata (West Bengal) are systematically lower—by 60 µg/m³ (39%) in January and 30 μg/m³ (44%) annually—compared to those recorded at the nearby US Air Now station. A model evaluation at Kolkata using only the US Air Now station data, instead of averaging across all available measurement stations, significantly reduces the positive model bias from 145% to 49% in January, and from 147% to 45% annually.

We then utilize satellite-derived AOD data to evaluate the model's performance in simulating the spatial distribution of aerosol column loadings across India. Satellite data provides greater spatial coverage than the surface $PM_{2.5}$ measurement network. WRF-Chem reproduces the spatial pattern of AOD, with a Pearson correlation coefficient of 0.84 between annual modeled and observed AOD across India (**Supplementary Figure 2**), and monthly correlations ranging from 0.72 to 0.82 (except for July when too much data is missing). However, WRF-Chem exhibits a consistent negative bias in AOD across India, with an annual mean bias (normalized mean bias) of -0.12 ± 0.06 ($-29 \pm 14\%$) compared to satellite observations. AOD underestimation persists even in regions where surface $PM_{2.5}$ concentrations are significantly overestimated (e.g., West Bengal). Previous modeling studies have attributed similar AOD underestimation over India primarily to the underrepresentation of large particles (diameter > 2.5 μ m) (David et al., 2018; Singh et al., 2021). Consistent with this, our simulation



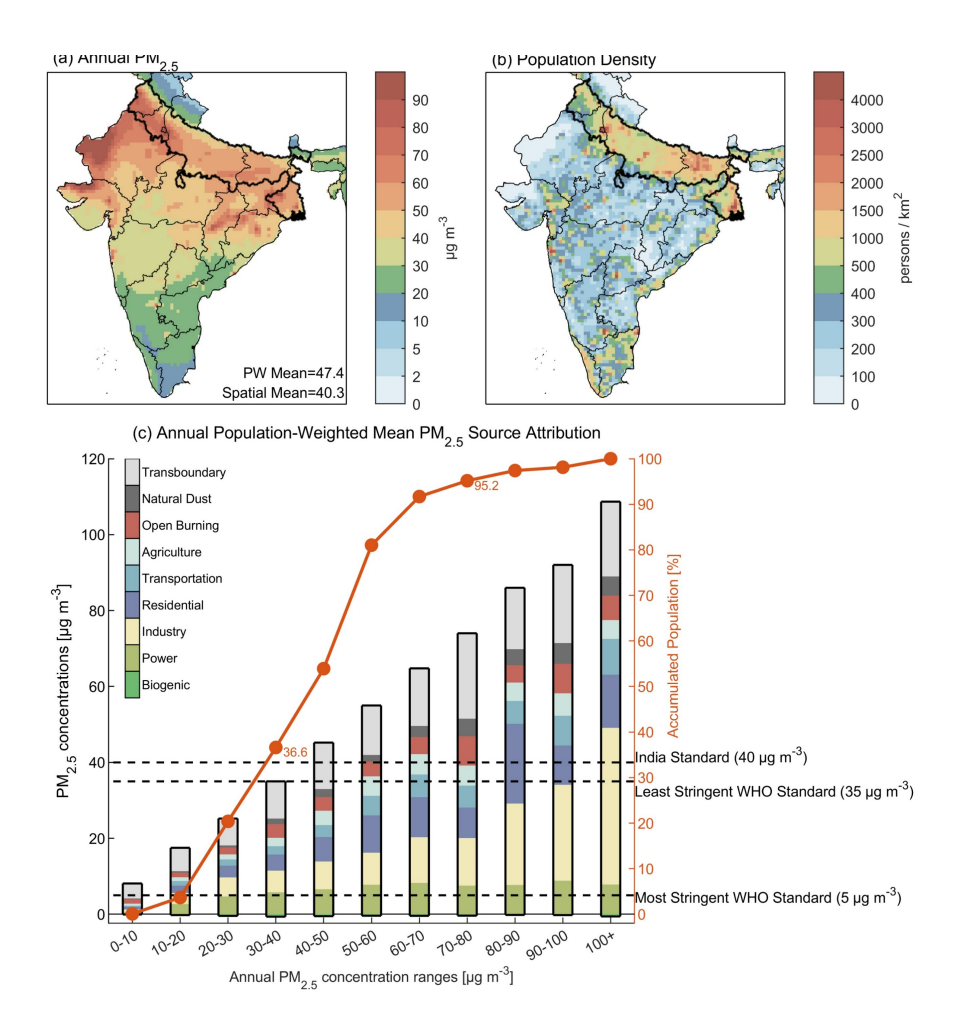
530



shows significantly underestimated surface coarse particulate matter (PM_coarse; particles with diameters > 2.5 μ m and \leq 10 μ m) compared to CPCB measurements (**Supplementary Figure 3**). This domain-wide low bias in PM_{coarse} concentrations is likely due to missing PM_{coarse} emissions (e.g., urban dust and other underrepresented burning activities) in our updated emission inventory.

3.3 Total surface PM_{2.5} concentrations and their source attribution across India in 2022

We analyze the national and regional surface PM_{2.5} concentrations (both total and attributed to specific sources) using the PW mean metric (see **Section 2.2.3** for PW mean calculation). PW mean concentrations reflect population exposure and is indicative of associated health risks. In addition, we investigate the spatial distribution of PM_{2.5} concentrations originating from various sources in order to identify local hotspots associated with specific emission sources.





545

550

555

560

565

570



Figure 5. Baseline annual PM_{2.5} concentrations in 2022 across India and their source attribution. In $\bf a$, Annual results are calculated as the average of January, April, July, and October simulations. Spatial distribution of annual average PM_{2.5} concentrations across India are shown in color. National averages for Population-Weighted (PW) and spatial mean PM_{2.5} concentrations are given as inset values in the figure. Panel $\bf b$ shows 27km² gridded population density across India. In $\bf a$ and $\bf b$, the thick black line denotes the boundary of the Indo-Gangetic Plain (IGP). In $\bf c$, WRF-Chem grids are aggregated by ranges of annual mean PM_{2.5} concentrations, with colored bars indicating source attribution (left Y axis). The red line and dots indicate the cumulative percentage of the population (right Y axis) living in areas where the annual mean PM_{2.5} concentration falls within or below a given concentration range. For example, 36.6% (95.2%) of the Indian population was exposed to annual PM_{2.5} concentrations < 40 (80) μ g/m³ in 2022). See monthly versions of panel $\bf c$ in Supplementary Figure 4.

Our WRF-Chem simulation estimates a 2022 national PW mean annual surface $PM_{2.5}$ concentration of 47.4 μ g/m³ (**Figure 5a**), similar to the 51.6 μ g/m³ reported in a recent satellite-based machine learning study (Kawano et al., 2025). In 2022, 37% of India's population lived in areas where annual $PM_{2.5}$ concentrations met the national air quality standard of 40 μ g/m³ (**Figure 5c**), representing an increase from 17% in 2016 (Apte and Pant, 2019). This change indicates an improvement in India's $PM_{2.5}$ air quality from 2016 to 2022 under the NCAP, aided by favorable meteorological conditions that enhanced pollutant dispersion and removal (Xie et al., 2024). However, in 2022, only 29% of the national population was exposed to $PM_{2.5}$ levels below the least stringent annual World Health Organization (WHO) standard (35 μ g/m³), and less than 0.1% met the most stringent annual WHO standard (5 μ g/m³). Regionally, the IGP experienced the highest annual PW mean $PM_{2.5}$ concentration in 2022 at 58.9 μ g/m³, followed by Northwest India (58.3 μ g/m³) and Central India (46.3 μ g/m³). In contrast, Northeast India (28.1 μ g/m³), South India (27.3 μ g/m³) and the Himalayan states (25.3 μ g/m³) had lower annual PW mean $PM_{2.5}$ concentrations.

At the national level, emissions originating within India accounted for 73% (34.5 μ g/m³) of the annual PW mean PM_{2.5} concentration in 2022, while transboundary emission sources contributed the remaining 27% (12.8 μ g/m³) (**Figure 6**). We summarize the national and state-level PW mean PM_{2.5} concentrations attributed by source in **Supplementary Table 5**.

Among domestic sources, the industrial sector was the leading contributor to the national annual PW mean $PM_{2.5}$ concentration in 2022, accounting for 18% (8.6 µg/m³). Spatially, its contribution was particularly dominant in heavily polluted areas where annual $PM_{2.5}$ levels exceeding 80 µg/m³ (twice the national standard) (**Figure 5c**). In some local hotspots within these areas—including major urban centers such those of Delhi and Mumbai—industrial emissions alone contributed more than 40 µg/m³ to simulated annual surface $PM_{2.5}$ concentrations (**Figure 6**), suggesting that to achieve national air quality standards in these hotspots it will be necessary to regulate industrial emissions.





India's residential sector, which has been undergoing a clean energy transition toward LPG since 2016, was the second-largest domestic contributor (15%; 7.3 μ g/m³) to the national PW mean PM_{2.5} concentration in 2022. Spatially, however, the residential sector remained the dominant PM_{2.5} source across large areas of the IGP, especially during winter (**Figures 7**). Consequently, ~500 million people in India lived in areas where residential emissions were the dominant source of annual PM_{2.5} pollution in 2022, the highest among all domestic sources. This highlights the continued substantial health burden associated with residential emissions, and the need to augment recent progress in adoption of cleaner cooking fuels.

580

585

575

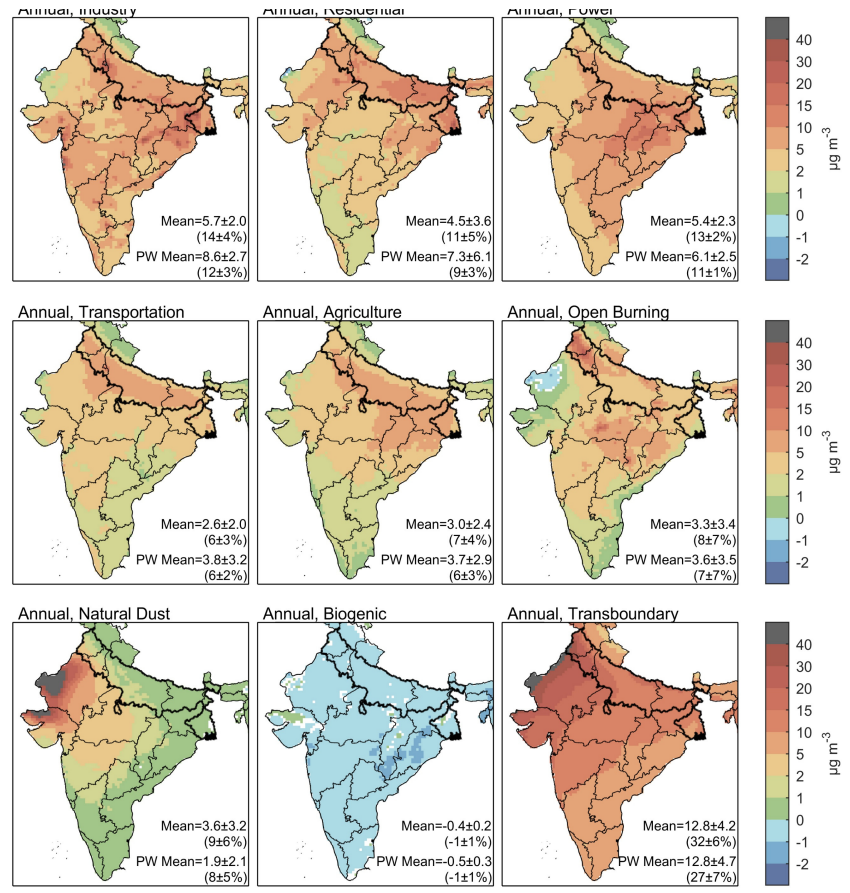


Figure 6. Spatial pattern of annual surface $PM_{2.5}$ concentrations across India in 2022 attributed to a given source. Annual results are calculated as the average of January, April, July, and October simulations. In each panel, numbers outside parentheses indicate the annual Population-Weighted (PW) mean $PM_{2.5}$ concentrations and spatial mean (Mean) $PM_{2.5}$ concentrations across India. Numbers inside parentheses represent the source's percentage contribution across India to total $PM_{2.5}$. Uncertainty bounds represent one standard deviation across monthly values, and provide an indication of the seasonal variation of a given sector's impact on surface $PM_{2.5}$. See **Supplementary Table 3** for source contribution to annual PW mean $PM_{2.5}$ at each state. The thick black line denotes the boundary of





the Indo-Gangetic Plain (IGP).

590

595

600

605

610

India's power sector, based on our updated emission inventory, was the third-largest contributor to the national PW mean PM_{2.5} concentration in 2022 (13%; 6.1 µg/m³). Spatially, the power sector primarily influenced PM_{2.5} air quality in Central India, particularly in Chhattisgarh and Jharkhand (Figures 6 and 7). This is due to central India generating 52% of India's annual coal-based electricity in 2022 and power plants typically having emission controls only on primary particulates and not on SO₂ or NO_x which contribute to the formation of secondary inorganic aerosols. About 270 million people lived in areas where power sector emissions were the largest domestic source for annual PM2.5 exposure. Notably, the spatial extent of power sector-dominated areas was the largest among all domestic emission sources.

India's transportation sector made a smaller contribution to the national annual PW mean PM_{2.5} concentration in 2022 (8%; 3.8 µg/m³), compared with the industry, residential, and power sectors. Spatially, its impact was most notable across much of the IGP and eastern Rajasthan, where it contributed moderately (~5 to 10 μg/m³)

to annual PM_{2.5} (Figures 5). In Delhi, the transportation sector recorded its highest state-level contribution to annual PM_{2.5}, reaching 11.6 µg/m³ (11%, Supplementary Table 5). However, transportation was not the

dominant domestic source of annual PM_{2.5} in any of India's populous regions in 2022 (Figures 6).

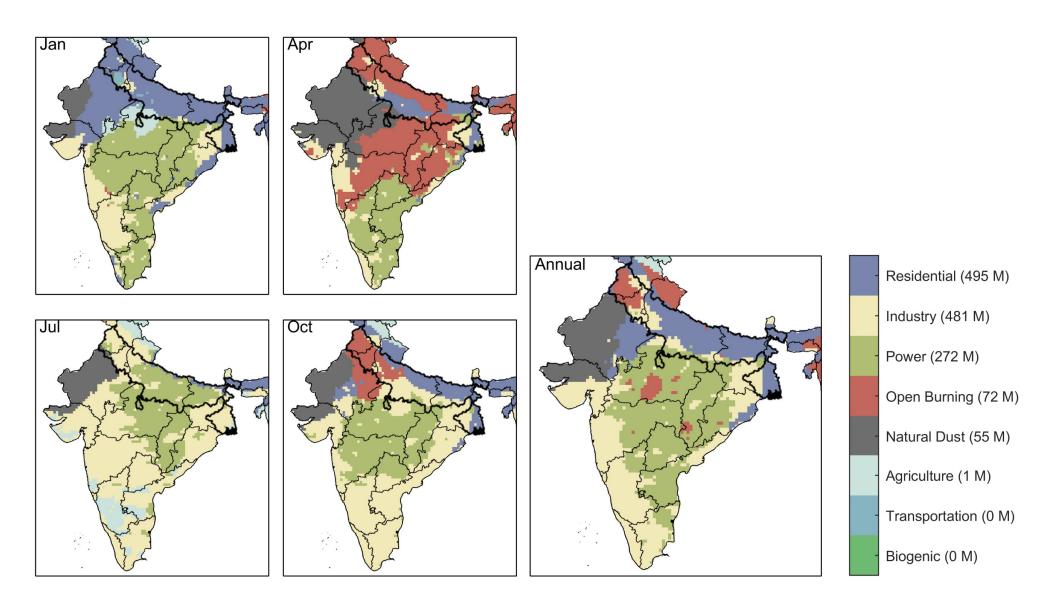


Figure 7. Dominant domestic PM_{2.5} sources at monthly and annual timescales. Transboundary emission sources are excluded. Numbers in parentheses in the legend indicate the population (in millions) across India residing in areas where a specific domestic emission source dominated in 2022. The thick black line denotes the boundary of the Indo-Gangetic Plain (IGP).



615

620

625



India's agricultural sources contributed 8% (3.7 $\mu g/m^3$) to the national annual PW mean PM_{2.5} concentration. This PM_{2.5} was primarily derived from secondary inorganic aerosols formed from NH₃ emitted from fertilizer use and livestock as well as a minor source from NO_x emitted from agricultural fields.

India's open burning emissions, derived from the FINN inventory and representing satellite- detectable burning of crop residues, municipal waste and wildfires, contributed 8% (3.6 μg/m³) to the annual PW mean PM_{2.5} concentrations across India in 2022. Their impacts were strongly seasonal, with elevated contributions of 15% (8.3 μg/m³) and 10% (4.3 μg/m³) to the national PW mean PM_{2.5} in April and October, respectively. Spatially, the regional hotspots switched between months. In April, open burning is most influential in Central India and Northeast India (**Figures 5**). In October, open burning became the dominant source of PM_{2.5} in northeastern IGP, including Delhi, with significant monthly contributions exceeding 40 μg/m³ (**Supplementary Figure 5**). Previous studies have shown that groundwater conservation policies in the northeastern IGP—one of India's major crop harvesting and residue burning regions—have shortened the turnover period between crop seasons and delayed agricultural burning (Balwinder-Singh et al., 2019). As a result, burning has shifted later in the year, often extending into late fall, when meteorological conditions are less favorable for pollutant dispersion, thereby amplifying the impact of open burning on surface PM_{2.5} concentrations (Liu et al., 2022). These earlier findings underscore the complexity of effectively controlling open burning emissions.

630

635

Domestic natural dust emissions, derived from desert dust simulated by WRF-Chem, contributed 4% (1.9 μ g/m³) to the national annual PW mean PM_{2.5} concentration in 2022. Spatially, it had a substantial impact on PM_{2.5} levels in Northwest India, where grid-level annual contributions exceed 40 μ g/m³ in its western part. However, due to the low population density in Northwest India and the limited impact of natural dust on surface PM_{2.5} outside this region (**Figures 4b** and **5**), natural dust was not a major factor for PM_{2.5} exposure at the national level. Despite limited exposure among the population, the natural dust zones overlap substantially with India's solar energy generation centers. This spatial coincidence may lower solar power generation efficiency due to aerosol-induced dimming and soiling, though the soiling impact can be mitigated if panels are cleaned on a regular basis (Li et al., 2020).

640

645

Domestic biogenic emissions had a small but net negative contribution to annual PW mean $PM_{2.5}$ concentrations across India (-1%; -0.5 μ g/m³). At the grid level, the net annual contribution was between -2 μ g/m³ to 0 μ g/m³ across the country. We find a reduction in secondary inorganic $PM_{2.5}$ components—sulfate, nitrate, and ammonium—as well as in the sulfate oxidation ratio and nitrate oxidation ratio, following the inclusion of domestic biogenic emissions in the WRF-Chem model (**Supplementary Figure 6**). The inclusion of biogenic VOCs reduced the atmospheric oxidation capacity by consuming OH and HO₂ radicals, thereby decreasing the conversion of SO_2 to sulfate and NO_2 to nitrate, which also reduced ammonium and led to reductions in secondary inorganic $PM_{2.5}$.



655

660

665



Transboundary sources (emissions from outside of India) accounted for 27% (12.8 μg/m³) of annual national PW mean PM_{2.5} in India in 2022, exceeding the contribution of any individual domestic emission source (**Figure 6**). These transboundary sources include emissions from six anthropogenic sectors (i.e., power, industry, residential, transportation, agriculture, and open burning) and three natural sources (i.e., dust and biogenic) from outside India, representing emissions beyond the jurisdiction of the Indian government. Spatially, the influence of transboundary sources exhibits a northwest-to-southeast gradient. In 2022, transboundary sources contributed more than 20% to grid-level annual PM_{2.5} concentrations across most of India, with contributions exceeding 30% in western states such as Punjab, Haryana, Rajasthan, and Gujarat (**Supplementary Figure 7**). In Delhi, transboundary sources contributed 21 μg/m³, or 20%, to the annual PM_{2.5} concentration in 2022.

3.4 Chemical components of total surface PM_{2.5} and their source attribution across India for 2022

We analyze the contributions of individual PM_{2.5} components simulated by WRF-Chem to total PM_{2.5} concentrations across India in 2022, along with their respective source attributions. **Figure 8** shows the spatial distribution of annual concentrations of all components. **Figure 9** and **Supplementary Table 6** present the source contributions to national PW mean concentrations of PM_{2.5} components.

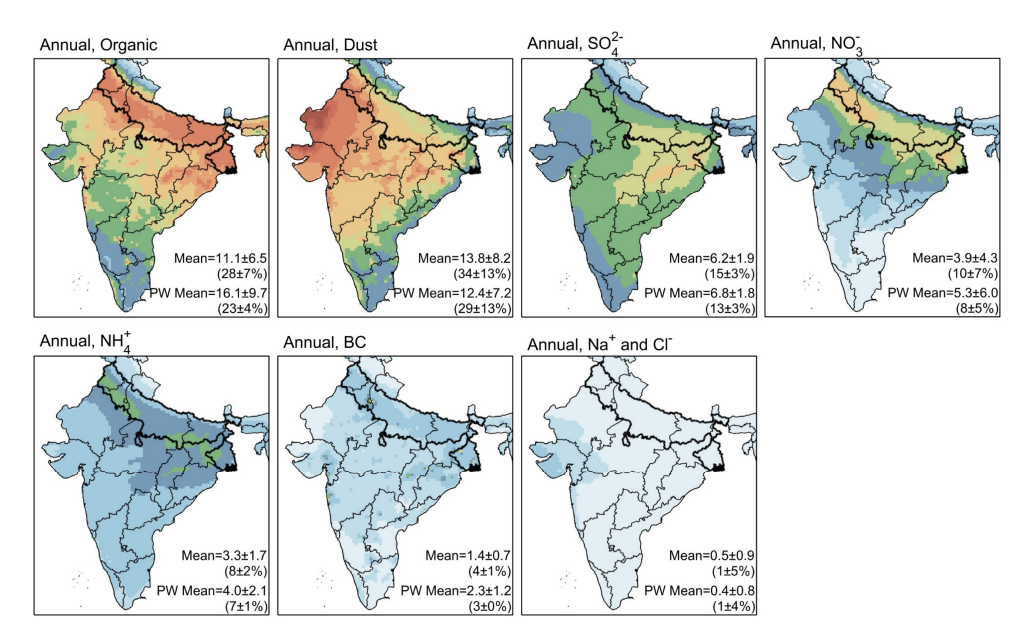


Figure 8. Spatial pattern of annual concentrations of PM_{2.5} components across India in 2022. Annual results are calculated as the average of January, April, July, and October simulations. In each panel, numbers outside parentheses indicate the Population-Weighted (PW) mean concentrations and spatial mean (Mean) concentrations across India. Numbers inside parentheses represent the component's percentage contribution to total PM_{2.5}. Uncertainty bounds represent one standard deviation across four monthly values representing each season. The thick black line denotes

670



680

685

690

695



the boundary of the Indo-Gangetic Plain (IGP).

Among components resolved by WRF-Chem, *organic* aerosols (including both primary and secondary) had the largest contribution to the national PW mean total PM_{2.5} concentrations in 2022, at 34% (16.1 μg/m³) (**Figure 8**). Residential emissions from within India were the dominant source of population exposure to organic PM_{2.5}, accounting for 6.6 μg/m³ of its annual national PW mean concentration (**Figure 9**). Transboundary (3.1 μg/m³) and industrial (2.6 μg/m³) sources were also significant contributors to organic PM_{2.5} levels across the country. Spatially, organic PM_{2.5} had a north-to-south gradient, with its dominance closely overlapping with regions where residential emissions were also dominant—particularly the IGP.

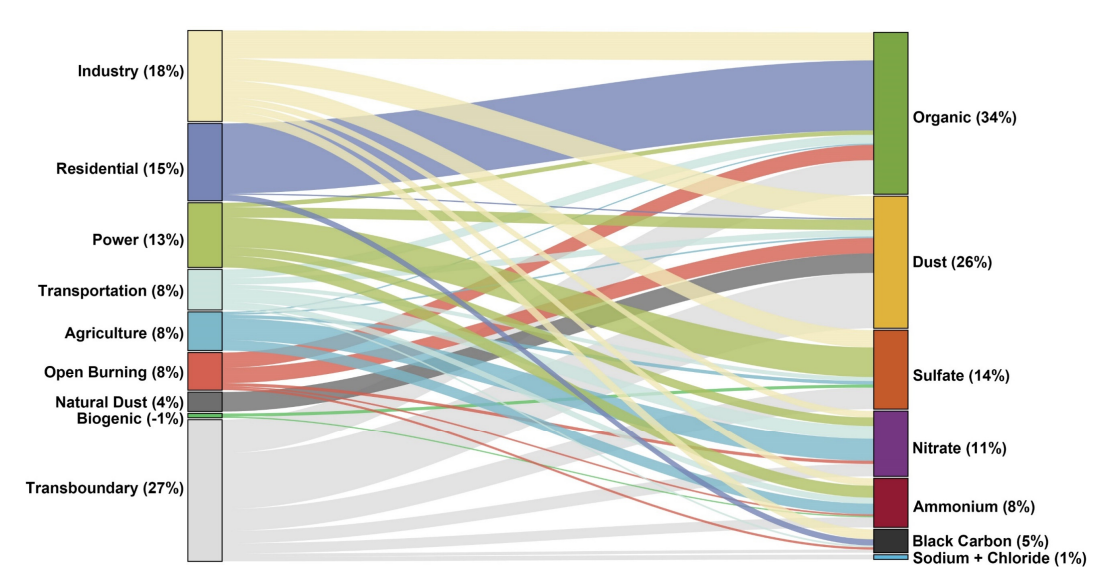


Figure 9. Source contributions to population-weighted mean concentrations of PM_{2.5} components across India in 2022. Contributions are attributed to six domestic anthropogenic sectors (industry, residential, power, transportation, open burning, and agriculture), two domestic natural sources (dust and biogenic emissions), as well as sources from outside of India (transboundary emissions). Note that contributions below $0.1 \mu g/m^3$ for a given source–component pair are omitted from the figure. All contributions presented are positive, except those from biogenic sources, which are negative. Numbers in parentheses indicate the percentage share (rounded to the nearest integer) of each source or component in the total PM_{2.5} concentration. See **Supplementary Table 6** for detailed values for each pair in this figure.

The dust component, including both anthropogenic and natural sources, was the second-largest contributor to the national PW mean total PM_{2.5} concentration in 2022, at 26% (12.4 μ g/m³) (**Figure 8**). Transboundary emissions dominated dust PM_{2.5} at the national level, contributing 5.0 μ g/m³ to its annual PW mean concentration (**Figure 9**). In addition, industrial (2.0 μ g/m³) and natural dust (1.8 μ g/m³) emissions from within India were the other major contributors to dust PM_{2.5} across India. Spatially, dust PM_{2.5} exhibited a west-to-east gradient, with





annual concentrations exceeding 40 µg/m³ across most of Rajasthan and Gujarat (Figure 8).

Sulfate PM_{2.5} was the third-largest contributor to the national PW mean total PM_{2.5} level in 2022, at 14% (6.8 μg/m³), and was the dominant component of secondary inorganic PM_{2.5} (including sulfate, nitrate, and ammonium) (**Figure 8**). India's power sector, the largest domestic SO₂ emitter, was the dominant source for sulfate, accounting for 2.8 μg/m³ of its annual PW mean concentration, followed by transboundary pollution and the industrial sector (**Figure 9**). Spatially, sulfate concentrations exhibited a relatively small gradient compared to organic and dust PM_{2.5}, though highest concentrations were found in eastern India around Chhattisgarh and Jharkhand.

705

710

715

720

725

730

700

Nitrate PM_{2.5} contributed 5.3 μg/m³ (11%) to national PW mean total PM_{2.5} concentration in 2022, smaller than that of sulfate PM_{2.5} (**Figure 8**). However, spatially nitrate PM_{2.5} was the dominant component among secondary inorganic PM_{2.5} across the IGP, especially in Bihar, Haryana, and Delhi. Unlike organic, dust, and sulfate PM_{2.5}, nitrate PM_{2.5} exhibited highly nonlinear relationships between precursor (i.e., NO_x) emissions and resulting concentrations. Specifically, the agriculture sector—contributing only 2% of national NO_x but 80% of national NH₃ emissions in 2022—were identified as the largest contributor (2.0 μg/m³) to nitrate PM_{2.5} in 2022 (**Figure 9**). In the atmosphere, nitric acid (HNO₃, from NO_x oxidation) reacts with NH₃ remaining after neutralizing sulfuric acid to form ammonium nitrate. Removing agricultural emissions reduced NH₃ availability across India by 77%, cutting the national average NO₃ fraction of total NO₃+HNO₃ from 51% (baseline) to 25% and leading to the largest nitrate reduction among all simulations that removed individual sources (**Figure 10**).

Ammonium $PM_{2.5}$ contributed 4.0 μ g/m³ (8%) to national PW mean total $PM_{2.5}$ concentration in 2022, with spatial hotspots overlapping those of sulfate and nitrate (**Figure 8**). Like nitrate, ammonium's response to precursor (NH₃) emissions was highly nonlinear. Notably, we identified India's power sector—emitting no NH₃ but 80% of national SO_2 and 40% of national NO_x emissions in 2022—resulted in the largest reduction (1.1 μ g/m³) of ammonium $PM_{2.5}$ when this sector's emissions were removed (**Figure 9**). While the power sector did not emit NH₃ directly, its dominance in SO_2 and NO_x emissions within India increased the availability of sulfuric and nitric acids, which react with NH_3 to form ammonium aerosols. Removing power sector emissions therefore left a larger fraction of total reduced nitrogen ($NH_x = NH_3 + NH_4^+$) as NH_3 , leading to greater reductions in ammonium $PM_{2.5}$ than any other single-source removal scenarios (**Figure 10**). In contrast, when removing agricultural emissions (dominant NH_3 source domestically), transport of NH_3 from outside India partially offset the decrease in NH_3 supply, sustaining some ammonium formation and leading to smaller reductions in ammonium than the simulation in which power-sector emissions were removed. These findings illustrate how when source emissions are entirely removed, non-linear chemistry can yield results that deviate from attributional methods (e.g., tagging precursor emissions) (Koo et al., 2009).

Black Carbon, primarily from the incomplete combustion of solid fuels, contributed 2.3 µg/m³ (5%) to



740

745



national PW mean total PM_{2.5} concentration in 2022, with India's industrial sector the dominant source.

Sodium and chloride together contributed only $0.4~\mu g/m^3$ (1%) to national PW mean total PM_{2.5} concentration in 2022, primarily from transboundary sources. Previous observational studies reported relatively high chloride concentrations in particulate matter in Delhi (e.g., 15-month average of 8.6 $\mu g/m^3$ during 2017-2018), Kanpur (e.g., monthly average of 19.3 $\mu g/m^3$ in January 2016), and Chennai (episodically), suggesting possible local emissions of hydrochloric acid from plastic-contained waste burning and industry (Gani et al., 2019; Thamban et al., 2019; Gunthe et al., 2021). However, because the emission inventories used in this study (i.e., CEDS, EDGAR, and FINN) do not include anthropogenic emissions of chloride-containing species, such elevated chloride levels observed in these cities were not reproduced in our model simulations. A recent modeling study that incorporated anthropogenic chlorine emissions reported a spatial average increase of 3–4 $\mu g/m^3$ in PM_{2.5} concentrations in the IGP during January–March 2018 (Patel et al., 2024). By comparison, our model simulated a spatial average of 88 $\mu g/m^3$ for January 2022 and 56 $\mu g/m^3$ for the annual mean in 2022 across the IGP, which suggests a relatively small impact of incorporating chlorine emissions into our source attribution studies.

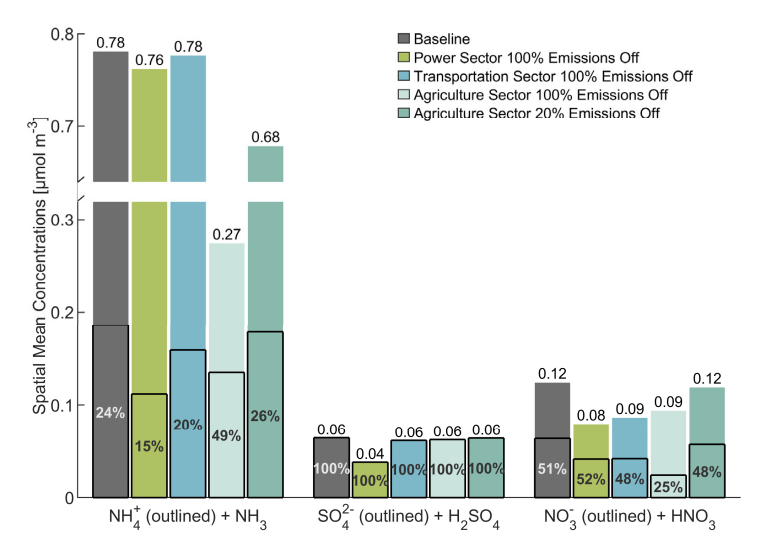


Figure 10. Partitioning between secondary PM_{2.5} components (NH₄⁺, SO₄²⁻, and NO₃⁻) and their relevant precursors (NH₃, H₂SO₄ and HNO₃) for the baseline simulation and following the removal of individual sectoral emissions. Annual spatial mean concentrations (in μmol/m³) across India in 2022 are shown for the baseline simulation (grey bars) and for scenarios where individual sector emissions (power, transportation, and agriculture) are removed completely or partially. Solid-line-outlined boxes indicate the concentrations of NH₄⁺, SO₄²⁻, and NO₃⁻, while the upper portions of each bar (above the outlined boxes) represent the concentrations of NH₃, H₂SO₄, and HNO₃. Numbers above each bar show the total concentration of the species group on the X-axis for the respective scenario. Percentages inside each outlined box indicate the share of NH₄⁺, SO₄²⁻, and NO₃⁻ in the total concentration of NH₄⁺+NH₃, SO₄²⁻





+H₂SO₄, and NO₃-+HNO₃, respectively.

760

765

770

775

780

4 Discussion

India's residential sector has undergone an energy transition with part of the sector moving from inefficient solid fuels to cleaner LPG, resulting in substantial reductions in primary PM_{2.5} emissions that would otherwise arise from biomass burning. The Pradhan Mantri Ujjwala Yojana (PMUY) program, launched in 2016, has played a central role by providing income support for LPG connections to rural and low-income households, and by December 2024 had reached over 103 million beneficiaries. Incorporating an updated residential inventory that captured this trend is key to our finding that the absolute and relative contributions of residential emissions to national population-weighted mean PM_{2.5} concentration are smaller than in two earlier studies for 2016 (Singh et al., 2021; Pai et al., 2022) (**Table 2**), though it remained the leading PM_{2.5} source in the IGP (**Figure 11**). In addition, our explicit separation of emissions from within and outside India further explains why our estimated residential contribution is smaller than in previous studies, which included transboundary residential sources when accounting for this sector (Conibear et al., 2018; Guo et al., 2018; Reddington et al., 2019; Chatterjee et al., 2023). However, recent research highlights challenges in sustaining LPG usage under PMUY, including high refill costs and subsidy delays (Asharaf and Tol, 2024; Gaikwad et al., 2025), which may result in backsliding to a continued reliance on solid fuels which may not be fully captured in the updated inventory.

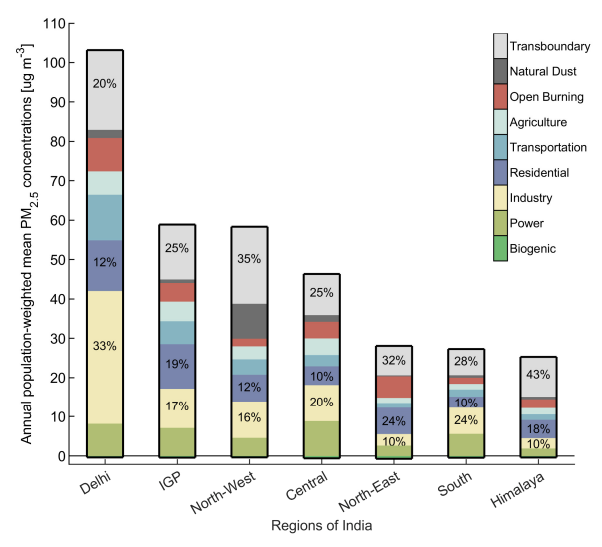


Figure 11. Source attribution of regional population-weighted mean annual PM_{2.5} concentrations in 2022 across Delhi and six regions of India. Inset numbers illustrate the percentage contribution from the largest three sources (including the transboundary source) in each region.



790

795

800



India's industrial sector emerged as the largest domestic contributor to India's PM_{2.5} pollution in 2022, resulting from rapid growth in activity and limited pollution controls. Specifically, its energy consumption nearly doubled from 7.8 EJ in 2010 to 13.6 EJ in 2022 with coal, biofuels, and waste being the dominant sources of energy (International Energy Agency, 2024), while emission regulations in this sector have primarily focused on improved energy efficiency with few new regulations focused on certain small-scale informal industries such as brick kilns (The Government of India, 2019; Tibrewal and Venkataraman, 2021). Consistent with these trends, the EDGAR global inventory reports an increase in primary PM_{2.5} emissions from the industrial sector from 1.4 Tg/year in 2010 to 2.1 Tg/year in 2022. Our adoption of the EDGAR 2022 inventory for the industrial sector therefore results in higher estimated absolute and relative industrial contributions to national population-weighted mean PM_{2.5} concentrations compared with earlier studies that focused on 2016 (**Table 2**). Notably, industrial sources contributed 33% of Delhi's annual PM_{2.5} in our analysis (**Figure 11**), a sharp increase from 14% in 2016 (Singh et al., 2021), underscoring the growing dominance of this sector in urban and national pollution burdens.

Table 2. A comparison of source attribution to national population-weighted mean PM_{2.5} concentration in India across studies[‡]

inula actoss studies								
		This Study	(Singh et al., 2021)	(Pai et al., 2022)				
Year	ı	2022	2016	2016				
Emission Inventory	Anthropogenic (excl. open burning)	CEDS _{v2024-07-08} for gas, EDGAR _{v8.1} for aerosols; Improved upon the residential and power emissions	Developed by the Greenhouse Gas and Air Pollution Interactions and Synergies (GAINS)- Asia model	$CEDS_{v2018-08}$, with NO_x and NH_3 emissions scaled using satellite observations				
	Open Burning	FINNv2.5.1		GFED4s				
Method		100% emissions off	20% emissions off	100% emissions off				
Source Attribution	Industry	18% (8.6 μg/m ³)	16%‡	$11\% (6.8 \mu g/m^3)$				
	Residential	15% (7.3 μg/m ³)	31%*	$21\% (12.9 \ \mu g/m^3)$				
	Power	13% (6.1 μg/m ³)	7% [‡]	19% (11.7 $\mu g/m^3$)				
	Transportation	8% (3.8 μg/m³)	7% [‡]	12% (7.4 μg/m³)				
	Agriculture	8% (3.7 μg/m³)	<12%**	14% (8.6 μg/m³)				
	Open Burning	8% (3.6 μg/m³)	8%‡	6% (3.7 μg/m³)				
	Transboundary	27% (12.8 μg/m³)	20%‡	<28% (17.2 μg/m³)¶				

[‡]In this table, we only include studies that investigated emissions from within India for a direct comparison with our results.

^{*}Agricultural NH₃ emissions were aggregated with other emission source as 'Others Source' in this study.

Transboundary sources were aggregated with natural emissions as 'Background Source' in this study.

[‡]This study did not report national population-weighted mean PM_{2.5} concentration attributed to a given source.



810

815

820

825

830

835



India's power sector has been heavily and increasingly relied on coal generation, with the challenges of implementing emission controls for SO₂ and NO_x. Coal-based electricity generation substantially increased from 658 TWh in 2010 to 1307 TWh in 2022 (International Energy Agency, 2024). Although the Indian government introduced stringent emission standards for thermal power plants in 2015, compliance has been weak, with only about 3% of coal-based plants having installed flue gas desulfurization (FGD) systems by 2022 (National Environmental Engineering Research Institute, 2024). As a result, SO₂ emissions from the power sector increased substantially between 2010 and 2022, with CEDS reporting a 34% rise and EDGAR a 71% rise, consistent with satellite-derived SO₂ total column concentration trends across India during this period (Xie et al., 2024). In addition, the adoption of NOx control technologies in India's coal-fired plants are being tested but are not yet commercially deployed as India's high-ash coals can adversely impact NO_x control systems (Wiatros-Motyka, 2019). Projections further suggest that with only limited adoption and operation of pollution-control technologies continuing, SO₂ emissions from the power sector could rise by nearly 500% between 2020 and 2050 (Venkataraman et al., 2018). These trends, combined with the recent suggested relaxation of FGD requirements for coal plants (Koshy, 2025), will likely increase secondary inorganic aerosol formation and will threaten to undermine national efforts to reduce PM_{2.5} pollution and protect public health. The plant-level database and emission inventory developed in this study provide a foundation to further evaluate the air quality and health benefits of a clean power transition for future studies.

Import of pollution across national borders (transboundary sources) continued to be responsible on average for over 20% of surface PM_{2.5} pollution in 2022, similar to findings from 2016 (**Table 2**). These results underscore the persistent influence of transported pollution on India's air quality.

Our source attribution approach has inherent limitations due to the nonlinear chemistry of secondary aerosol formation and aerosol–meteorology feedbacks, similar to previous studies that employed the complete source removal method (Conibear et al., 2018; Pai et al., 2022; Chatterjee et al., 2023). For example, we identify the power sector as the largest contributors to ammonium PM_{2.5} in 2022, despite the fact that it did not emit NH₃. This result is primarily driven by secondary inorganic aerosol chemistry (discussed in **Section 3.4**) and are consistent with findings from a previous study for 2016 (Pai et al., 2022). We also find a small but non-negligible contribution of agricultural emissions to national PW mean dust concentrations (0.15 µg/m³). This counterintuitive result reflects the impact of aerosol–meteorology feedbacks: when agricultural emissions are removed, reductions in secondary PM_{2.5} improve ventilation conditions by weakening aerosol–radiation interactions (Zhou et al., 2019), thereby lowering primary PM_{2.5} concentrations, even though their emissions themselves are unaffected. These examples illustrate the interpretive challenges inherent to source attributional results via complete emission removal.

Nonlinear secondary aerosol chemistry limits the direct application of our results to real-world emission



845

850

855

860

865

870

875



regulations, particularly for sources dominated by PM_{2.5} precursor emissions whose reductions have a nonlinear effect on resulting PM_{2.5} concentrations, since policies typically involve partial rather than complete reductions. For sources dominated by primary PM_{2.5} components, such as the industrial and residential sectors, the differences between complete removal and scaled partial reductions are small: national spatial mean and population-weighted mean PM_{2.5} concentration reductions differ by less than 7% and 3%, respectively, between a 100% emission reduction and a fivefold scaling of 20% reductions (**Supplementary Figure 8**). However, for the agricultural sector, a 20% emission reduction results in 25% less national PM_{2.5} reduction (after a fivefold scaling) compared with a 100% emission reduction. This nonlinearity is primarily due to India's overall NH₃-rich environment (**Figure 10**), where nitrate availability limits secondary inorganic aerosol formation. This suggests that partial removal of NH₃ is less effective—defined as concentration decrease per unit emission reduction—in mitigating PM_{2.5} than substantial NH₃ emission reductions.

5 Conclusion and Implications

We conduct the first WRF-Chem model evaluation and source attribution analysis for India for the year 2022, leveraging recent advances in India-specific residential and power sector emission inventories and the expansion of ground-based PM_{2.5} monitoring networks. Our simulations incorporate the 2022 CEDS and EDGAR global emission inventories (released in 2024), a 2022 coal-fired power plant emission inventory developed in this work, and a revised 2022 residential emission inventory (Velamuri et al., 2024). We also incorporate the simple SOA scheme into WRF-Chem and improve model treatment of near-surface mixing of pollutants. We evaluate the baseline WRF-Chem simulation against observed PM_{2.5} concentrations from 288 surface monitoring sites across India and neighboring countries, demonstrating very good model performance across India that captures spatial and temporal variations of PM_{2.5} concentrations in 2022. Our findings, compared with earlier source attribution studies, highlight that residential emissions from within India are no longer the largest source of national population-weighted mean PM2.5 pollution, although they remained the second-largest domestic contributor nationally (Figures 6 and 9) and the leading contributor regionally in the Indo-Gangetic Plain (Figure 11). Instead, industrial emissions from within India emerged as the largest domestic contributor at the national scale, while the power sector within India ranks third, with 77% of its contribution arising from secondary inorganic PM_{2.5} formed from gaseous precursor emissions. Importantly, transboundary sources contributed more than any individual domestic source to surface PM_{2.5} concentrations in 2022 across India.

Tracking India's evolving air pollution and the shifting contributions of various sources is needed to inform regulatory mitigation strategies. This requires robust air quality modeling based on up-to-date emission inventories that incorporate real-world changes in activity, emission factors, technology adoption, and regulations. By combining information from both global and regional inventories, our study provides an improved understanding of PM_{2.5} pollution and its source attribution for 2022, with several implications. First, efforts to reduce primary PM_{2.5} emissions from the residential sector have been beneficial and should continue through initiatives such as the NCAP and the residential PMUY programs. In addition, electrification of the





residential sector coupled with decarbonization of the grid can further help reduce air pollution emissions (Zhou et al., 2022). Second, enforcement of new stringent emission regulations targeting both primary PM_{2.5} and SO₂ are needed for the fast-growing industrial sector, especially in densely populated urban areas. Continuing to improve energy efficiency for large and energy-intensive industries such as steel production under the Perform, Achieve, and Trade (PAT) scheme will also be beneficial for mitigating primary PM_{2.5} and SO₂ emissions from the industrial sector (Ministry of Power, 2022). Third, SO₂ controls in the coal dominated power sector should be enforced to prevent further deterioration of air quality particularly as new coal power comes on-line. Finally, more stringent regulations of local emissions are needed in areas heavily influenced by transboundary pollution in order to meet air quality standards. Collaborative efforts, including data sharing and cross-border source identification between India and its neighboring countries would be beneficial in identifying opportunities to improve air quality within South Asia. Future Indian PM_{2.5} pollution and its source attribution research will benefit from the development of a multi-year, India-specific emission inventory with recent coverage to better support long-term air quality management.

890

895

900

905

910

880

885

Data and Code Availability

Surface PM_{2.5} measurements from the India CPCB network are publicly available at: airquality.cpcb.gov.in/ccr/#/caaqm-dashboard-all/caaqm-landing. Continuous PM_{2.5} data from the U.S. AirNow network are no longer accessible, and the daily quality-controlled PM_{2.5} concentrations used in this study will be shared at the Princeton archive at LinkTBD upon accepted for publication. The WRF-Chem source code can be obtained from: github.com/wrf-model/WRF/releases. The CEDS emission inventory is available at: github.com/JGCRI/CEDS. The EDGAR emission inventory is available at: edgar.jrc.ec.europa.eu/dataset_ap81. The HTAP emission inventory is available at: edgar.jrc.ec.europa.eu/dataset_htap_v31. Meteorological data from ERA5 are available at: ecmwf.int/en/forecasts/dataset/ecmwf-reanalysis-v5. Gridded population data were retrieved from: earthdata.nasa.gov/data/catalog/sedac-ciesin-sedac-gpwv4-popdens-r11-4.11. Annual result for WRF-Chem output generated in this study will be publicly available via the Princeton archive at LinkTBD upon accepted for publication. The MATLAB Script for Sankey plot in Figure 9 is publicly available at https://www.mathworks.com/matlabcentral/fileexchange/128679-sankey-plot. Geographical boundaries used in all map plots are adopted from a global database (https://doi.org/10.1371/journal.pone.0231866).

Author contributions

M.Z. and D.L.M. conceptualized the study. M.Z. incorporated the simple SOA scheme into WRF-Chem and updated the 2022 residential and power sector emission inventories with the help from M.N. V.V. and H.K. M.Z. performed the simulations. M.Z. and D.L.M. analyzed the results and wrote the manuscript. Y.X. contributed to model validation. All authors contributed to interpreting the findings and revising the manuscript.

Financial support





Mi Zhou and Yuanyu Xie acknowledge support from the M.S. Chadha Center for Global India at Princeton
University. Mi Zhou, Denise L. Mauzerall, and Yuanyu Xie acknowledge support from the Princeton School of
Public and International Affairs and its Center for Policy Research on Energy and the Environment.

Acknowledgements

We thank Ruqian Miao for assistance with implementing the simple SOA scheme in WRF-Chem. We are grateful to Edmund Downie for compiling the plant-coal source dataset, and Shivansh Bansal for the help in pre-processing coal-fired plant data. We thank Aaron van Donkelaar for providing post-processed gridded AOD data, and Gargee Goswami and Kirat Singh for sharing insights on India's coal plant emissions and current regulations. We thank Rohit Gupta for the insights on policy implications of our studies. We also thank Chien Nguyen for assistance in collecting CPCB surface air quality data for 2022, and Ajay S. Nagpure for providing constructive feedback on recent clean energy transition in India's residential sector.

Competing Interests Statement

The authors declare no competing interest.

930

945

950

920

925

Reference:

- [1] Agarwal, P., Stevenson, D. S., and Heal, M. R.: Evaluation of WRF-Chem-simulated meteorology and aerosols over northern India during the severe pollution episode of 2016, Atmospheric Chemistry and Physics, 24, 2239-2266, 2024. [2] Apte, J. S. and Pant, P.: Toward cleaner air for a billion Indians, Proc Natl Acad Sci U S A, 116, 10614-10616, 2019.
- 935 [3] Asharaf, N. and Tol, R. S. J.: The impact of Pradhan Mantri Ujjwala Yojana on Indian households, Econ Anal Policy, 84, 878-897, 2024.
 - [4] Balwinder-Singh, McDonald, A. J., Srivastava, A. K., and Gerard, B.: Tradeoffs between groundwater conservation and air pollution from agricultural fires in northwest India, Nat Sustain, 2, 580-583, 2019.
 - [5] Bhaskar, U.: NDA Ujjwala surpasses targets, provides 80.33 million LPG connections, 2019.
- 940 [6] Chapman, E. G., Gustafson, W. I., Easter, R. C., Barnard, J. C., Ghan, S. J., Pekour, M. S., et al.: Coupling aerosol-cloud-radiative processes in the WRF-Chem model: Investigating the radiative impact of elevated point sources, Atmospheric Chemistry and Physics, 9, 945-964, 2009.
 - [7] Chatterjee, D., McDuffie, E. E., Smith, S. J., Bindle, L., van Donkelaar, A., Hammer, M. S., et al.: Source Contributions to Fine Particulate Matter and Attributable Mortality in India and the Surrounding Region, Environ Sci Technol, 57, 10263-10275, 2023.
 - [8] Chowdhury, S., Dey, S., Guttikunda, S., Pillarisetti, A., Smith, K. R., and Di Girolamo, L.: Indian annual ambient air quality standard is achievable by completely mitigating emissions from household sources, Proc Natl Acad Sci U S A, 116, 10711-10716, 2019.
 - [9] Conibear, L., Butt, E. W., Knote, C., Arnold, S. R., and Spracklen, D. V.: Residential energy use emissions dominate health impacts from exposure to ambient particulate matter in India, Nat Commun, 9, 617, 2018.
 - [10] Crippa, M., Guizzardi, D., Muntean, M., Schaaf, E., Dentener, F., van Aardenne, J. A., et al.: Gridded emissions of air pollutants for the period 1970–2012 within EDGAR v4.3.2, Earth System Science Data, 10, 1987-2013, 2018.





- [11] Cropper, M., Cui, R., Guttikunda, S., Hultman, N., Jawahar, P., Park, Y., et al.: The mortality impacts of current and planned coal-fired power plants in India, Proc Natl Acad Sci U S A, 118, 2021.
- 955 [12] David, L. M., Ravishankara, A. R., Kodros, J. K., Venkataraman, C., Sadavarte, P., Pierce, J. R., et al.: Aerosol Optical Depth Over India, J Geophys Res Atmos, 123, 3688-3703, 2018.
 - [13] Ding, Y., Wong, J., Patel, S., Mallapragada, D., Zang, G., and Stoner, R.: A Dataset of the Operating Station Heat Rate for 806 Indian Coal Plant Units using Machine Learning, preprint, 2024.
- [14] Du, Q., Zhao, C., Zhang, M., Dong, X., Chen, Y., Liu, Z., et al.: Modeling diurnal variation of surface PM2.5 concentration over East China with WRF-Chem: Impacts from boundary layer mixing and anthropogenic emission, Atmospheric Chemistry and Physics, 2020.
 - [15] Emmons, L. K., Schwantes, R. H., Orlando, J. J., Tyndall, G., Kinnison, D., Lamarque, J. F., et al.: The Chemistry Mechanism in the Community Earth System Model Version 2 (CESM2), Journal of Advances in Modeling Earth Systems, 12, 2020.
- 965 [16] Fast, J. D., Gustafson, W. I., Easter, R. C., Zaveri, R. A., Barnard, J. C., Chapman, E. G., et al.: Evolution of ozone, particulates, and aerosol direct radiative forcing in the vicinity of Houston using a fully coupled meteorology-chemistry-aerosol model, J Geophys Res-Atmos, 111, 2006.
 - [17] Gaikwad, H. V., Pandey, S., Kadam, V., and Patil, K.: Socio-economic factors on choice of cooking fuel: understanding the antecedents and consequences of PMUY In India, Discov Sustain, 6, 2025.
- [18] Gani, S., Bhandari, S., Seraj, S., Wang, D. S., Patel, K., Soni, P., et al.: Submicron aerosol composition in the world's most polluted megacity: the Delhi Aerosol Supersite study, Atmospheric Chemistry and Physics, 19, 6843-6859, 2019.
 [19] Gettelman, A., Mills, M. J., Kinnison, D. E., Garcia, R. R., Smith, A. K., Marsh, D. R., et al.: The Whole Atmosphere Community Climate Model Version 6 (WACCM6), Journal of Geophysical Research: Atmospheres, 124, 12380-12403, 2019.
- [20] Ginoux, P., Chin, M., Tegen, I., Prospero, J. M., Holben, B., Dubovik, O., et al.: Sources and distributions of dust aerosols simulated with the GOCART model, Journal of Geophysical Research: Atmospheres, 106, 20255-20273, 2001.
 [21] Govardhan, G., Satheesh, S. K., Moorthy, K. K., and Nanjundiah, R.: Simulations of black carbon over the Indian region: improvements and implications of diurnality in emissions, Atmospheric Chemistry and Physics, 19, 8229-8241, 2019.
- 980 [22] Grell, G. A., Peckham, S. E., Schmitz, R., McKeen, S. A., Frost, G., Skamarock, W. C., et al.: Fully coupled "online" chemistry within the WRF model, Atmos Environ, 39, 6957-6975, 2005.
 - [23] Guenther, A., Karl, T., Harley, P., Wiedinmyer, C., Palmer, P. I., and Geron, C.: Estimates of global terrestrial isoprene emissions using MEGAN (Model of Emissions of Gases and Aerosols from Nature), Atmospheric Chemistry and Physics, 6, 3181-3210, 2006.
- [24] Guizzardi, D., Crippa, M., Butler, T., Keating, T., Wu, R., Kamiński, J. W., et al.: The HTAP_v3.1 emission mosaic: merging regional and global monthly emissions (2000–2020) to support air quality modelling and policies, 2025.
 [25] Gunthe, S. S., Liu, P., Panda, U., Raj, S. S., Sharma, A., Darbyshire, E., et al.: Enhanced aerosol particle growth sustained by high continental chlorine emission in India, Nature Geoscience, 14, 77-84, 2021.
- [26] Guo, H., Kota, S. H., Chen, K., Sahu, S. K., Hu, J., Ying, Q., et al.: Source contributions and potential reductions to health effects of particulate matter in India, Atmospheric Chemistry and Physics, 18, 15219-15229, 2018.
 - [27] Guttikunda, S. K. and Jawahar, P.: Atmospheric emissions and pollution from the coal-fired thermal power plants in India, Atmos Environ, 92, 449-460, 2014.
 - [28] Health Effects Institute: State of Global Air Report 2024, Health Effects Institute (HEI), 2024.



1020



- [29] Hoesly, R. M., Smith, S. J., Feng, L., Klimont, Z., Janssens-Maenhout, G., Pitkanen, T., et al.: Historical (1750–2014)
 anthropogenic emissions of reactive gases and aerosols from the Community Emissions Data System (CEDS), Geosci Model Dev, 11, 369-408, 2018.
 - [30] Huang, X., Ding, K., Liu, J., Wang, Z., Tang, R., Xue, L., et al.: Smoke-weather interaction affects extreme wildfires in diverse coastal regions, Science, 379, 457-461, 2023.
 - [31] Institute for Health Metrics and Evaluation: Global Burden of Disease 2021, 2024.
- 1000 [32] International Energy Agency: World Energy Outlook 2024, 2024.
 - [33] Katiyar, A., Nayak, D. K., Nagar, P. K., Singh, D., Sharma, M., and Kota, S. H.: Fugitive road dust particulate matter emission inventory for India: A field campaign in 32 Indian cities, Sci Total Environ, 912, 169232, 2024.
 - [34] Kawano, A., Kelp, M., Qiu, M., Singh, K., Chaturvedi, E., Dahiya, S., et al.: Improved daily PM(2.5) estimates in India reveal inequalities in recent enhancement of air quality, Sci Adv, 11, eadq1071, 2025.
- 1005 [35] Koo, B., Wilson, G. M., Morris, R. E., Dunker, A. M., and Yarwood, G.: Comparison of Source Apportionment and Sensitivity Analysis in a Particulate Matter Air Quality Model, Environ Sci Technol, 43, 6669-6675, 2009.
 - [36] Koshy, J.: Sulphur-cleaning device in coal plants not necessary: Central scientific committee, 2025.
 - [37] Kumar, A., Imam, F., Dixit, K., Chaudhary, E., Sharma, S., Singh, N., et al.: Sectoral Contributions to Primary and Secondary PM2.5 in Regional Airsheds of India, ACS Earth and Space Chemistry, 2025.
- 1010 [38] Kumar, M. and Dahiya, S.: Emission Watch: Tracking the implementation of emission standard notification for coal-based power plants in India, Centre for Research on Energy and Clean Air, 2023.
 - [39] Kurokawa, J. and Ohara, T.: Long-term historical trends in air pollutant emissions in Asia: Regional Emission inventory in ASia (REAS) version 3, Atmospheric Chemistry and Physics, 20, 12761-12793, 2020.
 - [40] Lelieveld, J., Evans, J. S., Fnais, M., Giannadaki, D., and Pozzer, A.: The contribution of outdoor air pollution sources to premature mortality on a global scale, Nature, 525, 367-371, 2015.
 - [41] Li, X., Mauzerall, D. L., and Bergin, M. H.: Global reduction of solar power generation efficiency due to aerosols and panel soiling, Nat Sustain, 2020.
 - [42] Liu, T., Mickley, L. J., Patel, P. N., Gautam, R., Jain, M., Singh, S., et al.: Cascading Delays in the Monsoon Rice Growing Season and Postmonsoon Agricultural Fires Likely Exacerbate Air Pollution in North India, J Geophys Res-Atmos, 127, 2022.
 - [43] Liu, Z., Zhou, M., Chen, Y., Chen, D., Pan, Y., Song, T., et al.: The nonlinear response of fine particulate matter pollution to ammonia emission reductions in North China, Environmental Research Letters, 2021.
 - [44] Lyapustin, A., Wang, Y. J., Korkin, S., and Huang, D.: MODIS Collection 6 MAIAC algorithm, Atmospheric Measurement Techniques, 11, 5741-5765, 2018.
- 1025 [45] Miao, R., Chen, Q., Shrivastava, M., Chen, Y., Zhang, L., Hu, J., et al.: Process-based and observation-constrained SOA simulations in China: the role of semivolatile and intermediate-volatility organic compounds and OH levels, Atmospheric Chemistry and Physics, 21, 16183-16201, 2021.
 - [46] Ministry of Power: Status of Implementation of National Mission for Enhanced Energy Efficiency (NMEEE) Three years of PAT Scheme constitutes of 7 cycles, 2022.
- 1030 [47] National Environmental Engineering Research Institute: Analysis of Historical Ambient Air Quality Data along with Emission from coal-based Thermal Power Plants for Developing a Decision Support System, 2024.
 - [48] Pai, S. J., Heald, C. L., Coe, H., Brooks, J., Shephard, M. W., Dammers, E., et al.: Compositional Constraints are Vital for Atmospheric PM(2.5) Source Attribution over India, ACS Earth Space Chem, 6, 2432-2445, 2022.
 - [49] Pai, S. J., Heald, C. L., Pierce, J. R., Farina, S. C., Marais, E. A., Jimenez, J. L., et al.: An evaluation of global organic



1050

1060

1065



- aerosol schemes using airborne observations, Atmospheric Chemistry and Physics, 20, 2637-2665, 2020.
 - [50] Patel, A., Reddy, M. C., Liu, P., and Gunthe, S. S.: Impact of Continental CI -N2O5 Multiphase Heterogeneous Chemistry on Regional Air Chemistry: A GEOS-Chem study over Indian Region 2024.
 - [51] Reddington, C. L., Conibear, L., Knote, C., Silver, B. J., Li, Y. J., Chan, C. K., et al.: Exploring the impacts of anthropogenic emission sectors on PM_{2.5} and human health in South and East Asia, Atmospheric Chemistry and Physics, 19, 11887-11910, 2019.
- [52] Schnell, J. L., Naik, V., Horowitz, L. W., Paulot, F., Mao, J., Ginoux, P., et al.: Exploring the relationship between surface PM2.5 and meteorology in Northern India, Atmospheric Chemistry and Physics, 18, 10157-10175, 2018.
 - [53] Sengupta, S., Adams, P. J., Deetjen, T. A., Kamboj, P., D'Souza, S., Tongia, R., et al.: Subnational implications from climate and air pollution policies in India's electricity sector, Science, 378, eabh1484, 2022.
- 1045 [54] Sharma, A., Venkataraman, C., Muduchuru, K., Singh, V., Kesarkar, A., Ghosh, S., et al.: Aerosol radiative feedback enhances particulate pollution over India: A process understanding, Atmos Environ, 298, 2023.
 - [55] Singh, K., Peshin, T., Sengupta, S., Thakrar, S. K., Tessum, C. W., Hill, J. D., et al.: Air pollution mortality from India's coal power plants: unit-level estimates for targeted policy, Environmental Research Letters, 19, 2024.
 - [56] Singh, N., Agarwal, S., Sharma, S., Chatani, S., and Ramanathan, V.: Air Pollution Over India: Causal Factors for the High Pollution with Implications for Mitigation, ACS Earth and Space Chemistry, 2021.
 - [57] Thamban, N. M., Joshi, B., and Tripathi, S. N.: Evolution of Aerosol Size and Composition in the Indo-Gangetic Plain: Size-Resolved Analysis of High-Resolution Aerosol Mass Spectra, ACS Earth and Space Chemistry, 2019.
 - [58] The Government of India: National Clean Air Program (NCAP), 2019.
 - [59] India Climate & Energy Dashboard: https://iced.niti.gov.in/energy/electricity/generation/fuel-linkage, last
- 1055 [60] Tibrewal, K. and Venkataraman, C.: Climate co-benefits of air quality and clean energy policy in India, Nat Sustain, 4. 305-+. 2021.
 - [61] U.S. Environmental Protection Agency: Bituminous And Subbituminous Coal Combustion,
 - [62] Velamuri, V., Nayak, D. K., Sharma, S., Parmar, P. D., Nagar, P. K., Singh, D., et al.: India leads in emission intensity per GDP: Insights from the gridded emission inventory for residential, road transport, and energy sectors, Journal of Environmental Sciences, 2024.
 - [63] Venkataraman, C., Brauer, M., Tibrewal, K., Sadavarte, P., Ma, Q., Cohen, A., et al.: Source influence on emission pathways and ambient PM2.5 pollution over India (2015-2050), Atmos Chem Phys, 18, 8017-8039, 2018.
 - [64] Venkataraman, C., Anand, A., Maji, S., Barman, N., Tiwari, D., Muduchuru, K., et al.: Drivers of PM2.5 Episodes and Exceedance in India: A Synthesis From the COALESCE Network, Journal of Geophysical Research: Atmospheres, 129, 2024.
 - [65] Wiatros-Motyka, M.: NOx control for high-ash coal-fired power plants in India, Clean Energy, 3, 24-33, 2019.
 - [66] Wiedinmyer, C., Kimura, Y., McDonald-Buller, E. C., Emmons, L. K., Buchholz, R. R., Tang, W. F., et al.: The Fire Inventory from NCAR version 2.5: an updated global fire emissions model for climate and chemistry applications, Geosci Model Dev, 16, 3873-3891, 2023.
- 1070 [67] Xie, Y., Zhou, M., Hunt, K. M. R., and Mauzerall, D. L.: Recent PM2.5 air quality improvements in India benefited from meteorological variation, Nat Sustain, 2024.
 - [68] Zaveri, R. A. and Peters, L. K.: A new lumped structure photochemical mechanism for large-scale applications, Journal of Geophysical Research: Atmospheres, 104, 30387-30415, 1999.
- [69] Zaveri, R. A., Easter, R. C., Fast, J. D., and Peters, L. K.: Model for Simulating Aerosol Interactions and Chemistry (MOSAIC), Journal of Geophysical Research, 113, 2008.





[70] Zhang, X., Xiao, X., Wang, F., Yang, Y., Liao, H., Wang, S., et al.: Discordant future climate-driven changes in winter PM2.5 pollution across India under a warming climate, Elem Sci Anth, 11, 2023.

[71] Zhou, M., Xie, Y., Wang, C., Shen, L., and Mauzerall, D. L.: Impacts of current and climate induced changes in atmospheric stagnation on Indian surface PM(2.5) pollution, Nat Commun, 15, 7448, 2024.

1080 [72] Zhou, M., Liu, H. X., Peng, L. Q., Qin, Y., Chen, D., Zhang, L., et al.: Environmental benefits and household costs of clean heating options in northern China, Nat Sustain, 5, 329-+, 2022.

[73] Zhou, M., Zhang, L., Chen, D., Gu, Y., Fu, T.-M., Gao, M., et al.: The impact of aerosol–radiation interactions on the effectiveness of emission control measures, Environmental Research Letters, 14, 2019.